Tampere University

EMMANUEL CHIMEZIE CHUKWU

# INVESTIGATING THE EFFECTS OF SUB-ANESTHETIC NITROUS OXIDE EXPOSURE ON EEG FEATURES

Faculty of Medicine and Health Technology (MET)
Supervisors: Prof. Jari Hyttinen | Dr. Narayan P. Subramaniyam
Master's thesis
March 2023

# Abstract

EMMANUEL CHIMEZIE CHUKWU: INVESTIGATING THE EFFECTS OF SUB-ANESTHETIC NITROUS OXIDE EXPOSURE ON EEG FEATURES
Master's thesis
Tampere University
Master's Degree Programme in Biomedical Sciences and Engineering
March 2023

---

The human brain has one of the most complex networks in the world. Neuroscience attempts to address this complexity by studying the function of the regular nervous system and the effects of neurological, neurodevelopmental, and psychiatric disorders. Major depressive disorder is a known clinical condition plaguing millions today. Some research seeks to give insight into the mechanisms and therapeutic processes of clinical depression. There has been some evidence that nitrous oxide relieves depression symptoms in some subjects, but little is known about how nitrous gas affects brain interactions after anaesthesia. In this work, continuous and intermittent EEG data of subjects induced with the gas were pre-processed to remove prevalent noise and separated into even window trials according to a pipeline. It was possible to evaluate the effects of the circumstances on brain connections since the weight phase lag index had the greater statistical power to identify phase synchronization alterations and was least sensitive to additional noise sources that are uncorrelated. Graph analysis of EEG data shows that nitrous oxide alters brain connectivity on a varied scale. The strength of these changes differs among the subjects and frequency bands considered, but all subjects' neural interactions were consistently altered by nitrous oxide. The effects of nitrous oxide on the EEG were evident in both groups, with some participants exhibiting increased delta connectivity values. After anaesthesia, a noticeable decline in beta band connection strength was observed in individuals in the continuous group. Small data size, sensor-level data and lack of preceding research are potential limitations of this work. With more participants, data points and source-level data analysis, a more comprehensive understanding of nitrous oxide's effect on the brain may be possible. This thesis does not, therefore, make any general assertions about the use of nitrous oxide as an antidepressant. However, the methods developed in this work will be beneficial in further study of this investigation.

**Keywords:** Nitrous oxide, EEG connectivity, depression.

# Preface

The thesis was written for Tampere University's master's degree program in Biomedical Sciences and Engineering, Health Technology and Informatics.

I was introduced to the subject of this thesis work in the masters' seminar course thesis role adverts with the Biophysics and Imaging research group at Tampere University under the supervision of Jari Hyttinen and Narayan Puthanmadam Subramaniyam. The work was also done in collaboration with the Department of Anesthesiology, Tampere University Hospital, Laboratory of Neurotherapeutics, Drug Research Program and the SleepWell Research Program Unit, University of Helsinki. I am grateful for the supervisors' guidance, assistance, and patience throughout this thesis work. I thank other members of the collaborative groups for the materials and indications shared in relation to the study protocol and the diverse knowledge shared.

Tampere, 2nd March 2023

Emmanuel Chimezie Chukwu

# Contents

# List of Figures

*Figures in this section derived from this thesis' algorithms and those from outside sources have been duly referenced and have the appropriate copyright permissions.*

# List of Tables

# 1 Introduction

The human brain is among the most intricate systems in the universe [1]. The scope of neuroscience seeks to provide insight into the brain state and consciousness and this has widened over time to involve various approaches used to study the nervous system at different scales. Neuroscientists have developed numerous techniques to study neurons, from molecular and cellular studies to imaging of motor, sensory, and cognitive processes. In order to develop therapeutic measures for neurological disorders, it is crucial to understand how the brain functions in various patient cases. Recent studies have used several noninvasive imaging modalities that aid the understanding of human brain function. Examples of imaging techniques that can deliver millimetre-level spatial resolution include positron emission tomography, single-photon emission computed tomography, and functional magnetic resonance imaging [2]. However, these methods have a temporal resolution disadvantage such that neuronal activities that occur in milliseconds can be lost. Alternatively, Electroencephalography EEG is a widely used and non-invasive method to monitor brain activity that has a high temporal resolution, based on electrical activity in the brain. EEG's millisecond temporal resolution makes it one of the ideal techniques for understanding the brain as a dynamic system [3]. In learning about the human brain, it is imperative to identify the source of an EEG signal. [4] indicated that this usually requires a source model, a head model and EEG data. He described the source model as a three-dimensional position of dipoles on the cortical surface and it is generally assumed that EEG signals are generated by sources that can be approximated as dipoles. He also mentioned that the head model helps to describe how the electric currents from these sources will flow through the head and finally end up as EEG measurements. Therefore, the electric forward head model is crucial for precise source localisation. This model involves determining the geometry, based on MRI data, and the conductivity of various tissue sections such as scalp, skull, cerebrospinal fluid, grey and white matter of the brain, etc. in the volume conduction process [2].

Psychiatric disorders such as major depression can be highly disabling and increase the risk of suicide, as well as contribute to the overall global disease burden [5]. In patients with depression, the N-methyl-D-aspartate receptor (NMDA-R) blocker ketamine quickly relieves symptoms [6, 7]. Nitrous oxide is a type of NMDA-R blocking dissociative anaesthetic that has recently been shown to relieve depression symptoms in some patients [8]. In a brain connectivity study using graph analyses by [9], nitrous oxide was found to induce changes in the brain network during anaesthesia, resulting in a decrease in information processing efficiency in cognition-

relevant frequency bands. Although research has been carried out on the sedative and depression-alleviation effect of nitrous oxide, there is still little scientific understanding in brain connectivity study of the effect of nitrous oxide to describe the features of the neuronal assemblies after anaesthesia. The depression-alleviating effect of nitrous oxide needs to be understood in terms of the interactions between brain regions. Connectivity is often analyzed to study the functional interactions of brain regions in both normal and pathological conditions. Thus, the concept of brain connectivity and some of its contemporary techniques explored in this work will give further insight into how nitrous oxide affects brain functions when subjects are anaesthetized.

This study retrieved EEG recordings without MRI data from 20 sub-anaesthetic-induced subjects. The data were divided into two groups, the continuous group and the intermittent group, based on the procedure given for the gas exposure. The continuous group procedure is 20min sub-anaesthetic gas exposure. The intermittent group procedure is two cycles of 10min followed by a 10min break. In both cases, considerations are made for the properties of the signal before, during and after the nitrous oxide-inspired process. Insights drawn from what happens to the features of the EEG before, during and after the gas exposure would be of clinical significance. This thesis will demonstrate how nitrous oxide affects brain function and how this depends on the timing method of exposure (intermittent or continuous). The methods applied shall provide tools for monitoring brain state and consciousness. All available information about the brain activity of the subjects comes from the EEG signals. This makes the exploration of EEG functional connectivity very important. Typically, electrophysiological connectivity is considered to reflect functional interaction due to the propagation of saltatory conduction through short-range volume conduction to individual electrodes [1]. It is unfortunate that the same volume conduction that enables EEG also creates difficulties for functional connectivity. In the practical use of EEG, long-range volume-conducted potentials reach multiple electrodes. This is the problem of volume conduction plaguing electrophysiology connectivity measures. Having only the EEG signals of the subjects, phase synchronization of brain connectivity metrics are found to be suitable in quantifying the interaction among neuronal groups of signals under consideration. To overcome the effect of volume conduction, studies have proposed various approaches. In this study, the weighted phase-lag index was used. The weighted phase-lag index was utilized due to its reduced sensitivity to additional, uncorrelated noise sources and its heightened ability to detect changes in phase synchronization [10]. This work will investigate the effect of nitrous oxide on four EEG frequency bands using the weighted phase-lag index connectivity measure. It will also compare this effect between the continuous and intermittent groups to provide an enhanced idea of how

nitrous oxide may be helpful in depression treatment.

The thesis is organized so that the objective and theoretical background knowledge are established before the methods and materials sections. The materials and methods describe the EEG dataset collection protocols, the raw EEG pre-processing pipeline and details of the implemented connectivity metric. This section also summarised the statistical techniques used to perform the analysis of the anaesthetic effect on the EEG features. The results section highlights the findings of the work presented in graphs and tables. These results are discussed in the next section, explaining the implication of the values obtained as a correspondence to other literature. Lastly, conclusions are presented on the key findings from the discussion and suggestions for future research are provided. Appendix A includes circular connectivity graphs not included in the results section, while Appendix B contains the script links used in this thesis.

# 2 Theoretical Background

The theoretical background for investigating neuronal interactions in event of anaesthesia employs a wide range of knowledge involving electrophysiology signal processing, and connectivity techniques. In this Chapter, the basics of EEG and its applications as well as measures of quantifying brain signals are presented.

## 2.1 Electroencephalography

EEG is a medical technique used to track the electrical activity of the cortex Figure 2.1, the outer layer of grey matter in the brain, which covers the inner parts. This activity is a result of action potentials [11]. In the cortex, regions are grouped based on the complexity of their functions in primary cortices and associated cortices. The brain produces several rhythmic patterns of electric impulses in different locations. A typical brain wave consists of five categories of frequency, inclusive of the delta, theta, alpha, beta and gamma bands. However, the scope of this work is limited to the first four of these frequency bands. The levels of these waves are relatively constant and similar among all normal individuals [12]. Certain neurological disorders, including seizures and brain lesions, can be diagnosed using brain waves.

It is essential to study EEG signals because they are used both for research and for studying brain functions. Various modalities, including invasive and non-invasive approaches, are used to quantify the characteristics of brain electrical activity. These methods can be deployed to understand, diagnose and treat brain diseases. As earlier stated, an EEG is one of the non-invasive methods used in the study of brain electrical activity. During an EEG, electrical signals produced in the brain can be picked up by small electrodes attached to the scalp. Measurements are made of the differences in the potentials of the electric fields caused by neural currents at the scalp. A more detailed description of this mechanism is found in the subsequent sections of this work.

### 2.1.1 EEG's biophysics and measurement

Scalp potentials originate from the intrinsic electrophysiological activities of the nervous system. By identifying the generator source(s) and electrical field(s) of propagation, one can identify the electrographic patterns that describe the expression of the brainwaves as normal or abnormal [14]. EEGs recorded at the scalp usually represent the collective electrical activity produced by many neurons in the region

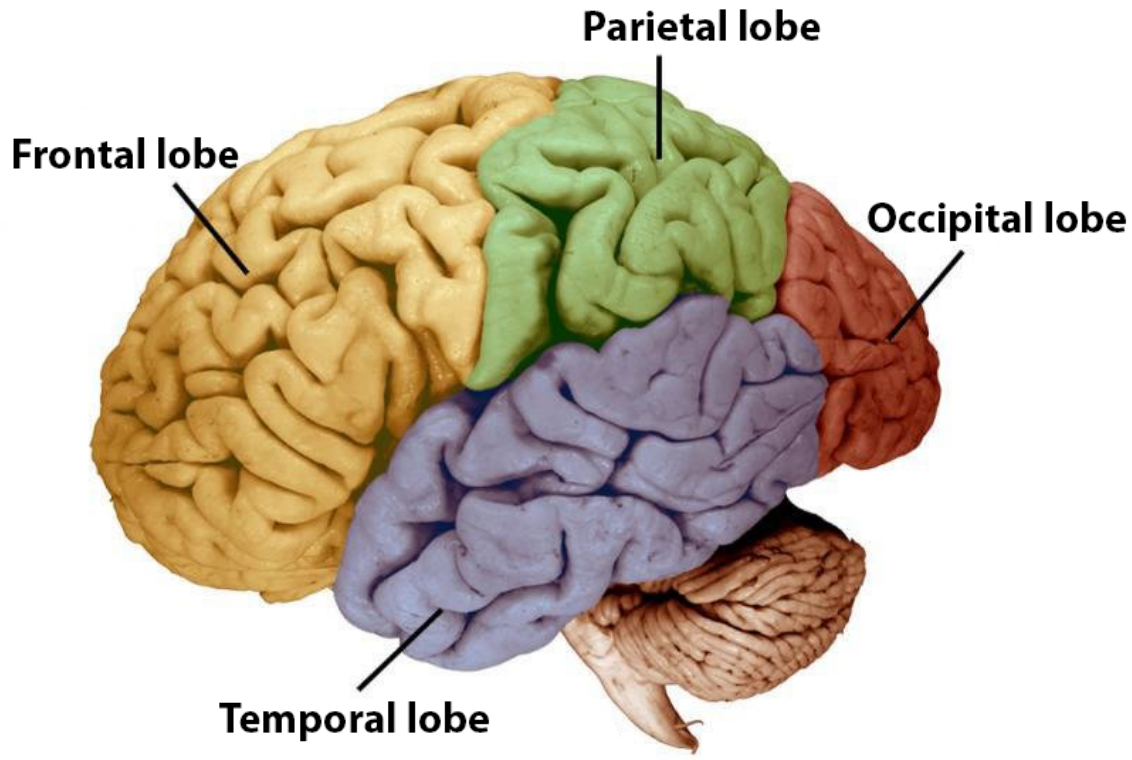


***Figure 2.1*** *The human brain cortex [13]*

and not action potentials [15]. The central nervous system creates electrical signals as electrical charges move. Ionic gradients established by neuronal membranes maintain normal neuronal function [14]. It is important to show a sufficient amount of electrical currents in the brain in order to be able to interpret the results of brain activity. Normally, resting (diffusion) membrane potential is maintained by the efflux of positive-charged potassium ions that maintain an electrochemical equilibrium of –75 mV. The depolarization process causes an influx of positive-charged sodium ions, which exceeds the resting potential of the electrochemical system to -55 mV [15]. These voltage changes determine how the lipid bilayer opens, and time determines how it closes. When the depolarization threshold is exceeded in the presence of conductance to adjacent nerve cell membranes, the ionic concentration change generates an action potential. EEG potentials, however, are primarily generated by synaptic potentials, which are the most significant source of extracellular current flow. Excitatory postsynaptic potentials (EPP) flow inward (from extracellular to intracellular) via sodium and calcium ions into other parts of the cell while the Inhibitory post-synaptic potential (IPP) which involves the chloride or potassium ions, flows outward (intracellular to extracellular) [14]. These postsynaptic potentials occur when neurotransmitters are released from the axon's terminal boutons at relatively slower rates[15]. EEG waveforms mainly consist of summed potentials

and they generally have a longer duration than the action potentials. In normal and abnormal situations, the brain stem and thalamus function as subcortical generators of synchronizing neocortical neurons. [14].

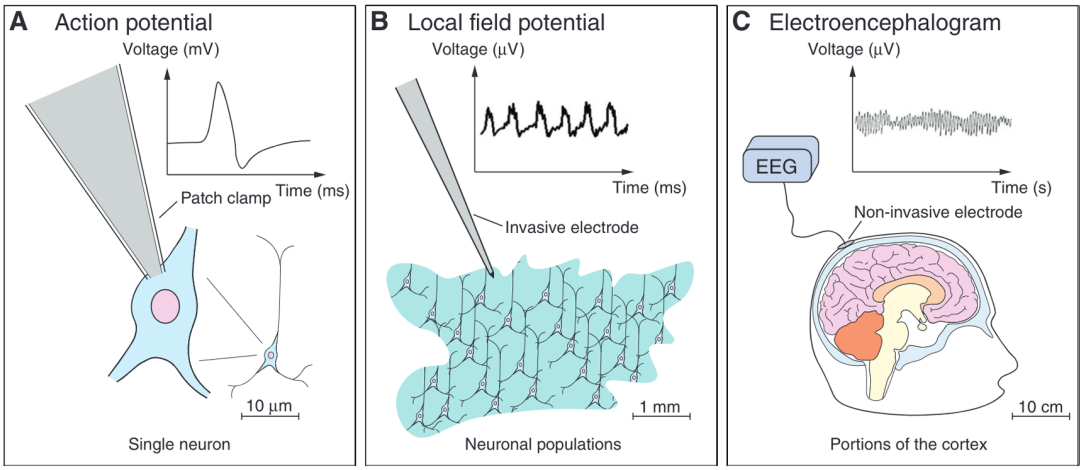


***Figure 2.2*** *Electrical activity of the brain measurement [15]*

A direct measure of neuronal activity can be performed by analyzing electrical signals from single neurons, populations of neurons, and parts of the cortex. As described in [15] (A) in Figure 2.2 shows the patch-clamp technique used in single-unit recordings of action potentials of individual neurons. This schematic shows a pyramidal neuron. Action potentials have a short duration of usually 1 ms and high-amplitude ( 100 mV) pulses. In (B) neuronal activity can be recorded via electrode microarrays inserted into brain tissue. By using different filter settings, one can isolate multi-unit activity (action potentials) or lower frequency local field potentials (LFPs), which have similar spectral characteristics to scalp-recorded EEG. (C) Electroencephalography (EEG) measures the electrical activity of large portions of the brain using electrodes placed on the scalp. In the EEG, oscillations are governed by neuronal populations that are synchronized or desynchronized. Furthermore, volume conduction between the scalp and various intracranial media causes attenuation and distortion of the scalp signal. In other words, the single-unit activity could be compared to one-on-one conversations with a coach, LFPs could be compared to capturing commentators at a live football match, and EEG could be compared to hearing the cheers of fans from outside the stadium.

An internationally recognized method for recording EEG that allows electrode placement to be standardized is the 10-20 system. This method ensures that inter-electrode spacing is equal and electrode placements are proportional to skull size and shape. It covers all brain regions shown in the Figure 2.3. The numbers are placed so that odd are on the left side and even on the right. The letter of the electrode indicates the general region of the brain that it covers. From front to back, the

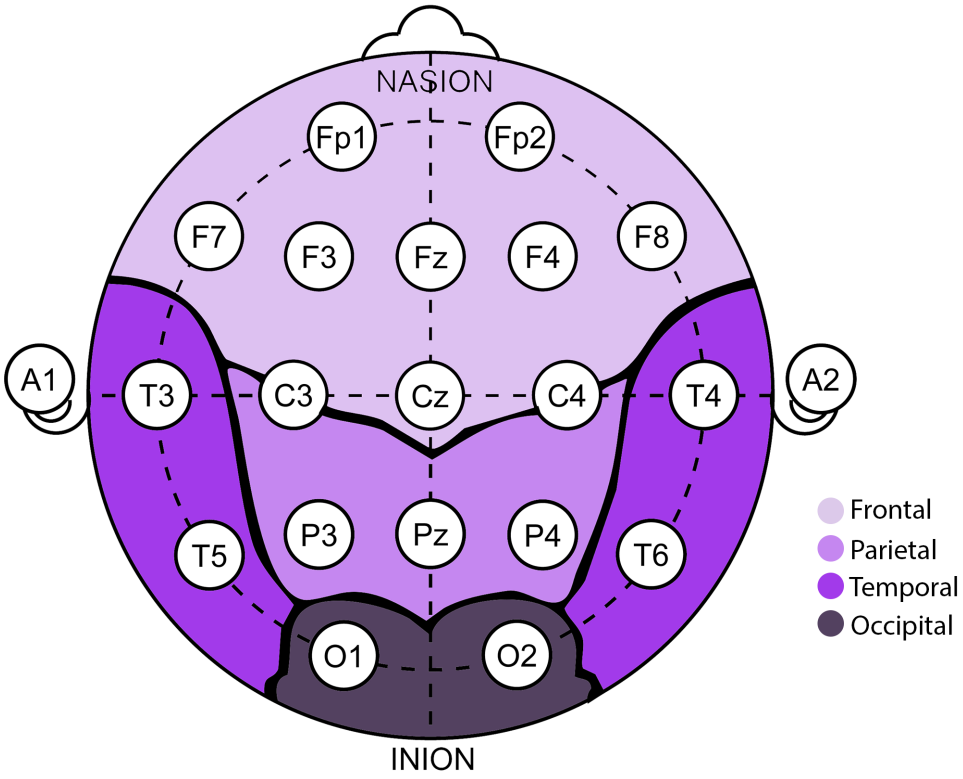


***Figure 2.3*** *The electrode layout in the corresponding brain regions of the 10-20 system (image generated from photo)*

electrodes are labelled as follows: Fp (frontal pole or pre-frontal), F (frontal), C (central brain line), T (temporal), P (parietal) and O (occipital). The higher-dimension EEG systems have electrodes lying between these lines combining multiple letters and ordering from front to back. Additionally, the letters M and A are referred to as the mastoids or earlobes respectively and are typically included to serve as an (offline) reference for signal analysis [16].

### 2.1.2 EEG Wave bands

EEG signals are broadly categorized into the delta, theta, alpha, beta and gamma. However, the description of the typical wave band characteristics for this study is as follows.

- **Delta wave**
  Delta wave is a low-frequency wave ranging up to 4 Hz. These waves tend to have the highest amplitude and slowest speed. They normally occur during deep sleep in all ages of patients. It is also seen normally in infants still developing [12]. This condition may be focally present with subcortical lesions as

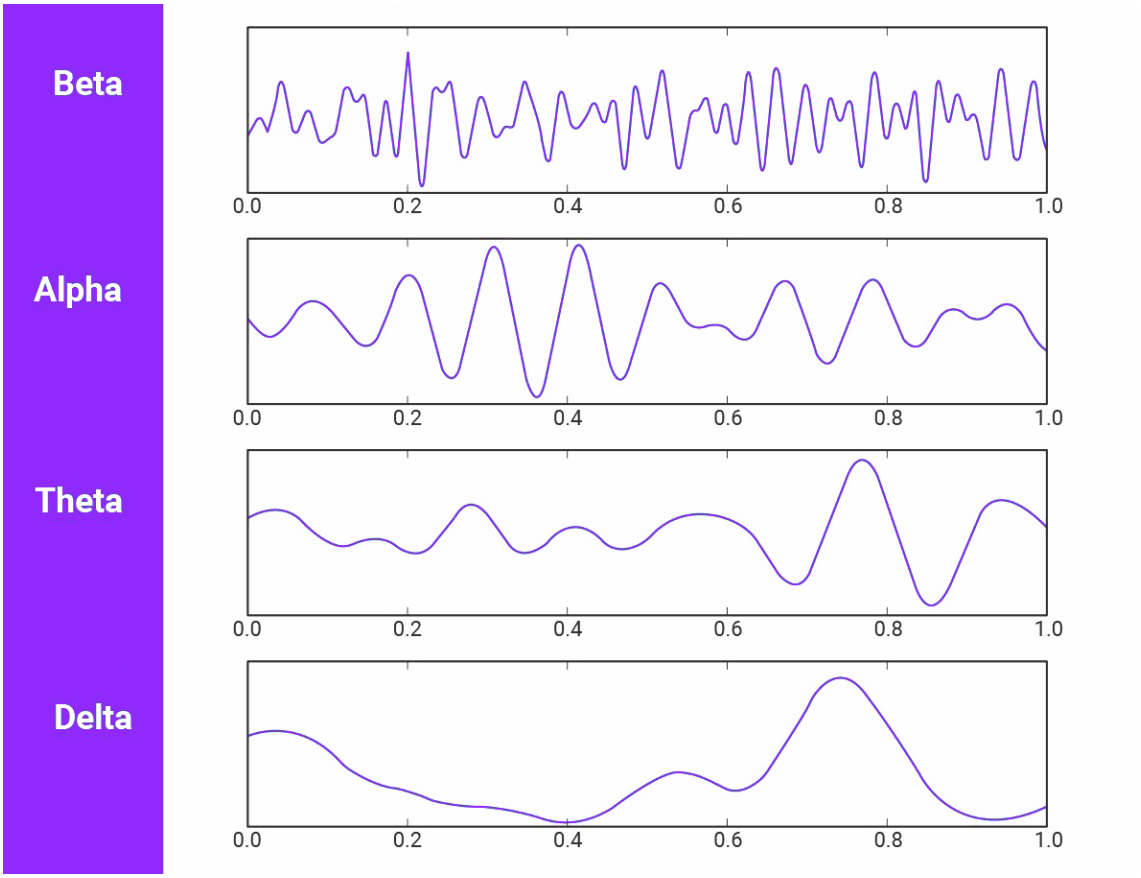


***Figure 2.4*** *EEG brain wave bands [17]*

well as in a diffuse manner with diffuse lesions, metabolic encephalopathy hydrocephalus, or deep mid-line lesions. It tends to be more prominent frontally in adults.

- **Theta waves**
  The theta band ranges from 4 - 8 Hz. Theta is commonly observed in young children whereas, among older children and adults, it can be manifested in drowsiness, arousal and in meditation [12]. A high theta value for the age indicates abnormal activity. In focal subcortical lesions, it can be seen as a focal disturbance seen in diffuse disorders or metabolic encephalopathy, in deep mid-line disorders, or in hydrocephalus in some instances. The opposite has been found to be true; reports of relaxation, meditative states, and creative thinking have been associated with this range.

- **Alpha waves**
  Alpha is an EEG rhythmic activity that could range from 8 - 12 Hz. Adults who are healthy and awake experience alpha waves when they are resting with their eyes closed. In the course of sleep and when concentrating on a particular task they disappear. Neurologists usually measure the alpha rhythm while a

patient's eyes are closed. The rhythm emerges when the patient closes their eyes and relaxes and diminishes when they open their eyes or exert themselves mentally [12].

- **Beta waves**
  At the time of attention to tasks or stimuli, beta waves replace alpha waves and are of a higher frequency. A person can experience them while concentrating, under stress, or when under psychological tension [12]. Beta waves usually have a rhythm between 12 - 40 Hz. Additionally, beta waves are present over the other frontocentral regions of the scalp, besides the regions described under alpha waves. Opening the eyes or beginning mental activity causes the alpha waves to decrease or attenuate, and beta waves to substitute for them.

### 2.1.3 EEG Applications

EEG devices can measure electrical activity associated with mental health states, thoughts, and imagination. These devices are used by researchers in diverse areas of research. EEG data applications are shown in Figure 2.5 along with their respective subcategories.

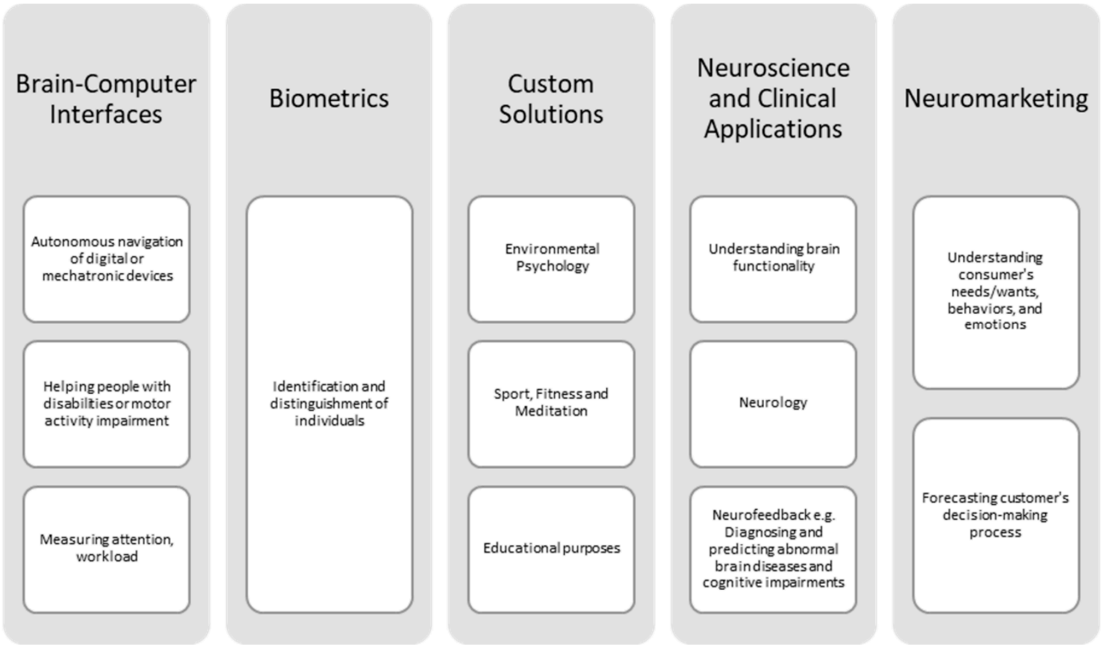


***Figure 2.5*** *Applications of Electroencephalography [18]*

#### Brain–computer interfaces (BCI)

A common application of EEG is in BCIs. They control and direct mechanical and electronic devices using real-time EEG data [19]. BCI devices allow individuals

with mild to severe motor disabilities to interact with machines, including those who are incapable of communicating with others [20]. Devices designed for the disabled use brain stimulation rather than muscle movement; they translate specific mental activities, such as imagining doing an activity, into control functions and commands [20, 21].
The list below shows examples of the most common BCI applications.

- Autonomous Navigation of Devices: This includes managing and monitoring sensors in smart homes [22], guiding and operating a drone [23], a vehicle dashboard [24], or a robot [25].
- Neurogaming and Entertainment: Involves controlling virtual reality (VR) or video games using body gestures and eye movements [26] and manipulating fiber optic dresses [27].
- Providing assistance to people with disabilities or impairments of motor activity: includes control of prosthetic arm [20], electrical wheelchair movement directing [28], using VR in post-stroke motor rehabilitation [29] and other purposes.

### Biometrics

Biometrics refers to the use of physiological and behavioural characteristics, like fingerprints, face, gaze, voice, iris, posture and gait to identify and distinguish people [30]. According to studies, EEG data can help reveal individual differences. In recent years, brain activity has been utilized for biometrics by using EEG data to identify individuals [31]. There are various reasons why EEG biometric systems have gained popularity, including privacy concerns, resilience against spoofing attempts, and universality [30, 31].

### Custom Solutions and Neurofeedback

In other research areas, EEG devices have been used to improve learning, well-being, and quality of life [18]. In both clinical and non-clinical research, neurofeedback data can be used to create custom EEG solutions in the following listed ways:

- Educational purposes: Evaluating cognitive workload and concentration levels while solving math puzzles, as well as confusion levels during online lectures with the goal of designing intelligent tutor systems [18]. It is applicable in the measurement of students reading ability. The visualization of the brain in real-time is also useful for educational purposes, training, and entertainment [32].

- Fitness, sports and meditation: Utilizing brain activity while exercising and listening to music to improve health status and quality of life [33].

### Neuroscience and Clinical applications

It is the goal of neuroscience to understand how the nervous system functions. In this way, clinical or non-clinical researchers can learn how the brain behaves and works when humans experience different emotional or mental states. Hence, according to [18], researchers use EEG devices in their studies across many fields as follows.

1. Cognitive neuroscience:
   In this field, cognitive load is measured, differences in brain wave activity between suicidal and non-suicidal states are analyzed, and brain activity during insight is examined. Learn how to analyse brain workload during decision-making, while learning new tasks, and also examining sleep patterns.

2. Behavioral neuroscience:

   - Measuring brain alertness in response to workplace lighting
   - Measuring mental workload of deaf children exposed to a noisy environment during a word recognition task
   - Detecting drowsiness or sleepiness in drivers and pilots
   - Evaluating stress level of surgeons during operations
   - Reducing stress levels
   - Environmental psychology.

3. Neurology:
   Real-time EEG data provides information on brain activity. EEG is used for diagnosing and predicting various abnormal brain diseases and cognitive impairments such as:

   - Level of consciousness
   - Neurosurgery
   - memory problems (e.g. Alzheimer's)
   - Parkinson's Disease
   - Language impairments (e.g. dyslexia)
   - Seizures and epilepsy
   - Attention Deficit Hyperactivity Disorder
   - Sleep disorders and insomnia

- Post-traumatic stress disorder
- Anxiety
- Traumatic brain injury (TBI)
- Multiple sclerosis diagnosis
- Amyotrophic lateral sclerosis
- Schizophrenia
- Autism in adults and children

4. Neurophysiology:
    - Fatigue detection
    - Measurement of brain activity after alcohol intake

**Neuromarketing or Consumer Neuroscience**

Today, neuromarketing has been added as one of the branches of the advertising industry. It is targeted at understanding consumer needs, emotions, and behaviours, and predicting their decision-making processes [34, 35]. Some neuromarketing research attempts to understand customer preferences and expectations regarding a specific product [34, 18] and their reaction to TV advertising by analyzing EEG signals.

## 2.2 Overview of Brain Connectivity Metrics

Recognizing changes in brain activity and the relationships between brain regions has grown in significance for examining both normal and abnormal brain function [36]. Grasping the operation of the brain involves more than simply recognizing the active areas, it requires comprehending the functional connections between neural networks throughout the brain [36]. The concept of brain connectivity is introduced to describe the relationship between brain areas. Structural and functional connectivity are examples of ways these activities can be quantified. Common metrics deployed in brain functional connectivity are described in this section. Functional connectivity could be subdivided based on if the metric measures the direction of cortical information flow or not. The measure of functional connectivity that is non-directed attempts to measure information interdependence without considering the direction of influence. Conversely, directed measures aim to establish causal relationships from the data based on the principle that causes come before their effects. With methods like Granger causality and transfer entropy, one can predict to some extent how effects will emerge. [37]. Both directed and undirected estimates can

further be distinguished into model-based and model-free approaches. According to [37], all the model-based approaches assume a linear kind of interaction taking place between two signals. Meanwhile, to quantify non-linear neuronal interactions, it may be useful to deploy model-free approaches. Some major metrics used in functional connectivity analysis are described as follows.

### 2.2.1 Dynamic Causal Modelling

Dynamic Causal Modelling (DCM) is a method of modelling the response of a dynamic system as a network of interacting neural sources, described in terms of conductance-based models or neural masses [36]. In EEG analysis, DCM entails the inversion of informed spatiotemporal models of observed responses. By varying only a few key parameters among conditions, modelling condition-specific responses over channels and peri-stimulus time is possible [38]. It is thus possible to apply this same approach to the analysis of single trials, where parameters can be modulated parametrically to model the changes in an experimental variable from trial to trial (e.g., reaction time or forgotten vs. remembered). The method can also be applied to steady-state source-reconstructed LFP, MEG or EEG responses under certain assumptions about the input distribution [38].

### 2.2.2 Granger Causality

Granger causality (GC) is a data-driven technique for analyzing connectivity. Unlike other methods, it does not require a specific model or prior information about spatial and temporal relationships [36]. Historically, GC was applied in the time domain, but in 1982, Geweke [39] applied it to the frequency domain to study EEG frequency bands. Over time, GC was extended from bivariate to multivariate signals [40, 41]. The Directed Transfer Function (DTF) and Partial Directed Coherence (PDC) are more recent offshoots of the GC method. In bivariate cases, DTF and PDC are equivalent, but in multivariate cases, PDC can identify both direct and indirect pathways between interacting brain regions. PDC is based on partial coherence [42], which evaluates the correlation between two signals out of n and addresses the issue of volume conduction in traditional coherence by considering the impact of interactions from $n - 2$ signals [36]. PDC measures directional influences as a continuation of partial coherence, which will be discussed further in the next section.

### 2.2.3 Coherence

The coherence metric evaluates pairs of signals in each frequency band using a correlation coefficient, which gauges the consistency of their relative amplitudes and phases [37]. Coherence quantifies linear phase synchronization and the extent

to which one signal can account for the other signal's variance, as a function of frequency, similar to the squared correlation coefficient in the time domain [43]. Simply put, the cross-spectral density of two signals, $i$ and $j$, at frequency $f$ can be expressed as;

$$Coh_{ij}(f) = \frac{|S_{ij}(f)|}{\sqrt{S_{ii}(f)S_{jj}(f)}} \tag{2.1}$$

Where $S_{ij}(f), S_{ii}(f)$ and $S_{jj}(f)$ are cross-spectral values from a singular matrix. The numerator term represents the length of the vector average of the individual trial cross-spectral densities between the signals at $f$ frequency. The divisor represents the square root of the product of the average of the individual trial power estimates of the signals at $f$ frequency [37].

Wavelet Coherence (WC) is a method of calculating coherence that uses a different approach. To achieve the best time-frequency resolution, it is necessary to know the coupling range in both time and frequency beforehand. WC is a function of time and scale that is mapped to specific frequency bins, referred to as pseudo frequencies. Calculating the leading dominant frequency of the scaled wavelet basis function is a necessary step in the mapping process [36]. WC uses a longer window for lower frequencies and a shorter window for higher frequencies, making it ideal for quantifying time-varying coherence [36].

Recently, the imaginary component of the coherence has gained popularity, particularly in the study of connectivity in EEG and MEG [37]. This component is obtained by projecting the complex-valued coherency onto the imaginary axis [3]. By discarding contributions to the connectivity estimate along the real axis, this method eliminates any instantaneous interactions that may be present due to field spread.

### 2.2.4 Phase Synchronization

Brain connectivity can be assessed using EEG in time, frequency or time-frequency domains. However, phase synchrony is calculated from the frequency domain representation of two signals. The concept of phase synchrony involves quantifying the consistency of the distribution of phase differences between single observations, which is based on the probability distribution of cross-spectral densities. To combine these densities, a weighted sum is taken that combines all vectors from head to tail and normalizes the result. If the phase difference between the two signals is consistent, the weighted sum length will be non-zero. However, if the phase differences are evenly distributed, the weighted sum will be close to zero [37]. This idea is demonstrated in Figure 2.6.

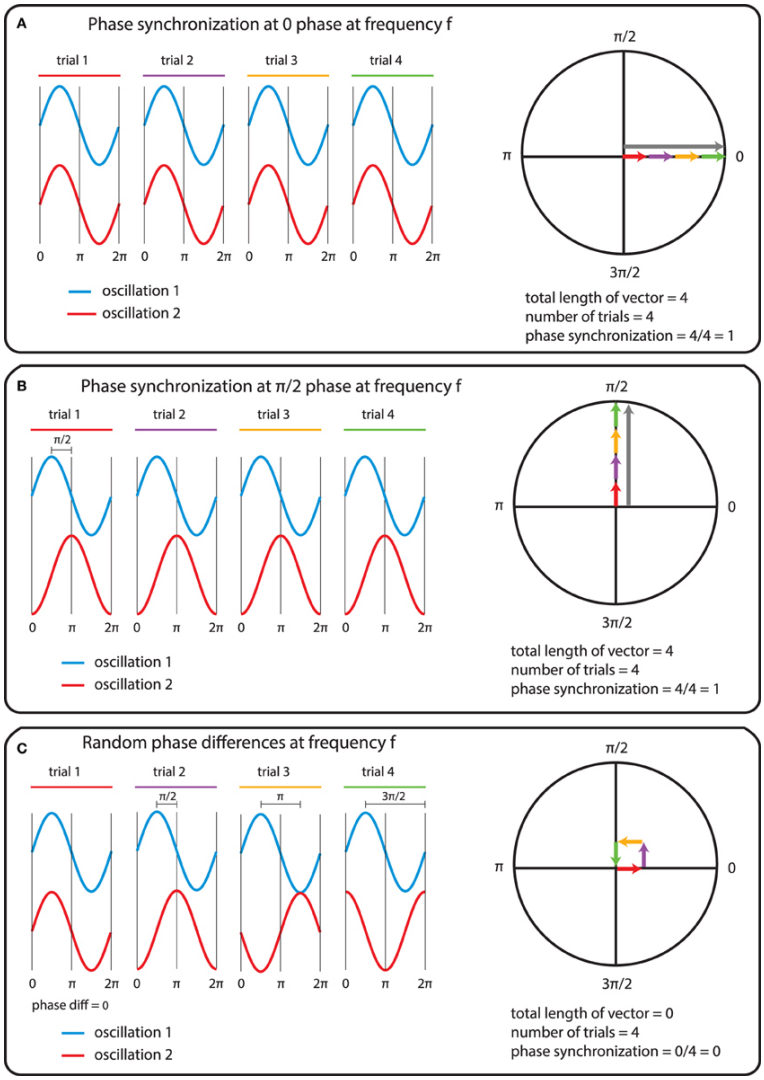


***Figure 2.6*** *Measure of synchrony computation: (A) A perfect phase alignment at 0 radians. (B) A scenario of complete synchronization with a radian variance of π/2. (C) No phase synchronization due to inconsistent phase differences [37]*

.

Assuming oscillation 1 and oscillation 2 are two signals with amplitudes of 1 and divided into four trials, Figure 2.6A shows that a vector sum with a length of 4 is obtained due to the same phase difference observed in all the trials. In the second scenario, the phase difference is consistent across observations at 90°. However, in Figure 2.6C, the phase differences are not consistent across trials, with differences of 0°, 90°, 180° and 270° for each trial. This results in cross-spectral density vectors pointing in different directions, which leads to a zero-length vector sum, indicating a lack of consistent phase difference. It is worth noting that in real data, the phase synchronization will fall between zero (vector sum equal to zero) and perfect synchronization (vector sum equal to 1) due to sampling size bias [37].

Interactions between neuronal groups result in phase synchronization that is mea-

surable from EEG, LFP or MEG signals [10]. Phase synchronization metrics like Phase Locking Value (PLV) and Phase Lag Index (PLI) are commonly used to analyze inter-regional functional connectivity. PLV is a phase-based connectivity method that considers only the instantaneous phases of signals and eliminates the ambiguity of coherence by ignoring the amplitude component[44]. If two regions are functionally connected, PLV assumes that their signal phase difference will remain relatively constant. Phase locking is computed by first filtering the instantaneous phase of signals since its physical interpretation is only done for narrow band signals [45]. PLI, on the other hand, measures connectivity based on the asymmetry of the distribution of phase differences between two regions. The idea here is, If there is consistent phase lag, it means there is a time lag between two-time series [37]. In other words, PLI shows how well brain regions are connected functionally when pairs of signals are synchronized. Unlike PLV, the main approach here disregards phase differences that centre around 0 mod  [46]. PLI values can range from 0 to 1, with 0 indicating possible non-coupling and 1 indicating complete phase locking. Despite PLI's advantage of being less affected by volume conduction and phase delays, its discontinuous characteristics inhibit the sensitivity to noise, volume conduction, and ability to detect phase-synchronization changes. A slight perturbation could turn phase leads into lags and vice versa. To address this, Vinck et al.[10] introduced the weighted phase lag index (wPLI) which has been used in the study.

### 2.2.5 Weighted Phase Lag Index

To introduce the Weighted Phase Lag Index (wPLI), it is necessary to compare it with the PLI connectivity measure. The formulae for PLI and wPLI are given Equation 2.2 and 2.3 respectively. In these equations, the cross-spectral density between two signals $i$ and $j$ is represented by $X_{ij}$. If the phase difference is equal to $n\pi$, the imaginary part of the cross-spectral density is 0, and if it is equal to $n\pi$ + $\pi/2$, where $n$ is an integer, the imaginary part is at its maximum. In the given equations, $sgn$ refers to the sign function and $I$, is the imaginary component.

$$PLI = |E[sgn(I(X_{ij}))]| \tag{2.2}$$

$$wPLI = \frac{|E[I(X_{ij})]|}{E[|I(X_{ij})|]}, \tag{2.3}$$

For PLI, a value greater than 0 indicates that there is an imbalance in the likelihood that the signal will be leading or lagging, while a value of 0 indicates that the signal leads and lags equally often. Signal only leads or only lags other signals if the value is 1.

A number greater than 0 indicates that there is an imbalance between these weights, whereas a value of 0 indicates that the total weight (not the quantity) of all leading relationships matches the total weight of lagging relationships. Similar to PLI, a value of 1 indicates that a signal solely leads or only lags another signal.

The wPLI is a tool for evaluating phase synchronization based on the imaginary components of the cross-spectrum. The metric is based on the PLI discussed previously and it is intended to increase the ability to reduce the impact of noise and phase shifts and increase the accuracy of detecting actual changes in phase synchronization [10]. In order to alleviate the discontinuity constraint of PLI, it uses the imaginary component of the cross-spectrum to weigh the contributions of observed phase leads and lags. In addition to their ability to detect true phase synchronization changes, the wPLI is also more sensitive to additional, uncorrelated noise sources compared to the PLI.

PLI and wPLI differ primarily in how phase relationships are weighted. In PLI, phase differences are weighted as $-1$ or 1 according to their sign. Phase differences in wPLI are weighted based on their values, which means that phase differences close to $\pm\pi 2$ are weighted more heavily than those closer to 0 or any other multiple of $\pi$. Consequently, all phase differences near this transition are treated similarly, avoiding discontinuities at the transition between positive and negative phases. As a result, the estimation of connectivity is more robust against outliers and noise. EEG/MEG recordings, for example, can be distorted by volume conduction, when multiple sensors on the scalp pick up the same neural signal. The relative phase differences between two signals can be reduced to zero, which affects connectivity estimation. The wPLI approach minimizes the contribution of phase relationships that are minor but non-zero (and may therefore be attributed to volume conduction), whereas PLI weighs these in the same way as phase relationships of $\pm\pi 2$ [47].

## 2.3 Nitrous oxide in Anesthesia

Nitrous oxide $N_2O$ is a sub-anaesthetic that is widely used for conscious sedation in medicine and dentistry [48]. Having the least potency of any inhalation anaesthetic, it can however not produce general anaesthesia alone, so it is used today primarily to reduce the quantity administered during general anaesthesia by using it as an adjunct [48]. As an example of a standard anaesthetic, nitrogen oxide in conjunction with ether anaesthetics, such as sevoflurane, desflurane, or isoflurane, and a muscle relaxant and analgesic is used [49]. The ether anaesthetic is typically switched to nitrous oxide during the closure of the surgical incision so that general anaesthesia recovery can be expedited. It produces insensibility to pain which is

maybe preceded by mild hysteria when inhaled. Studies have found that anaesthesia causes a decrease in the interconnection between brain regions[9] and most strongly in the parietal areas [50]. An analysis of nitrous oxide's effect on the brain network was conducted using graph theory, revealing that nitrous oxide interferes with information integration in cognitive and attention-related frequency bands. The disruption of the brain network during nitrous oxide administration may be linked to its sedative mechanism [9].

## 2.4 Statistical Significance

Statistical significance refers to the likelihood that a result or relationship observed in a sample is real and not due to chance. In hypothesis testing, a result is considered statistically significant if it is unlikely to have occurred by chance and provides evidence to support the hypothesis being tested [51]. More specifically, a study's defined significance level, denoted by alpha ($\alpha$), indicates how likely it is that the study will reject the null hypothesis if it is true [52]. The p-value of the result indicates the likelihood that the study will obtain at least as extreme a result. It is possible to define statistical significance as either strong or weak. When analyzing a data set and performing the required tests, it is important to support results with strong statistical significance and not simply assume they are a result of chance. A small p-value, often less than 0.05, means that the result is more reliable [51]. It shows that there is a significant difference between the two groups of data under consideration, hence, aiding a decision to reject a null hypothesis that claims the data groups are similar.

Considering multiple comparisons is a primary concern in EEG connectivity statistics. In EEG cap setups with more than 64 electrodes, there is the possibility for electrode pairs to assess connectivity within numbers greater than a thousand since the number of electrode pairs increases with the number of electrodes that are available to be analyzed. It is almost impossible to avoid false positives if multiple comparisons are not taken into account when statistical comparisons are made between experimental groups for every set of electrodes [53]. Common methods for controlling multiple comparisons are the Bonferroni correction and False Discovery Rate (FDR), but these methods can reduce statistical power, create overly strict values, and mask actual effects from adjusting the p-values for these two methods. The number of comparisons cannot be accurately accounted for by functional connectivity analysis and the Bonferroni correction assumes too much independence between electrode pairs [54, 55]. This is because EEG data is correlated and multidimensional, making functional connectivity values between different electrode pairs not independent.

# 3 Materials and Methods

The purpose of this chapter is to describe the materials and methods used to study the effects of nitrous oxide on EEG features. Materials presented in this article have been reviewed carefully in order to gain a better understanding of neuronal interactions after anaesthesia.

There are two groups of EEG data considered in this thesis: continuous and intermittent data. To meet the aims of this study, the data were pre-processed to remove prevalent noise and separated into even window trials according to the pipeline described in Section 3.2. Specifically, this study aimed to determine whether nitrous oxide affected EEG features after anaesthesia. The weighted phase lag index (wPLI) was used to check the effects of the conditions on neuronal interaction. In the sections that follow, we will describe the tools used and the steps that were taken in order to achieve our results.

## 3.1 Data Collection

The EEG data were collected from 20 healthy adult volunteers (all males, 18 - 40 years, BMI 18 -27). All subjects reported no medication/chronic illness and no previous history of psychiatric, neurological, or substance abuse disorder. Male volunteers were recruited because of the low incidence of nausea and also because of the menstrual cycle's effect on the EEG. The experiment protocols were compliant with the Helsinki declaration, and each subject provided written informed consent before the experiment. Before drug administration, the functions of monitors and data acquisition equipment were confirmed. Inhalation masks were placed and the participant breathed air through them for a few minutes. Next, the participant was asked to close their eyes and continue breathing steadily. An anesthesiologist adjusted the inspired nitrous oxide concentration (oxygen ad 100%) according to one of the following protocols (pre-randomization, see below):

**Study protocols**

Intermittent group (N=10):
Face mask trial 5 min ($O_2$ 100 %) $\rightarrow$ 50 % $N_2O$ 10 min $\rightarrow$ 100 % $O_2$ 10 min $\rightarrow$ 50 % $N_2O$ 10 min $\rightarrow$ 100 % $O_2$ 10 min.

Continuous group (N=10):
Face mask trial 5 min ($O_2$ 100 %) $\rightarrow$ 50 % $N_2O$ 20 min $\rightarrow$ 100 % $O_2$ 20 min.

Data were collected in each subject's folder and these folders contained multiple raw EDF files of the EEG recordings. It was possible to concatenate these EDF files

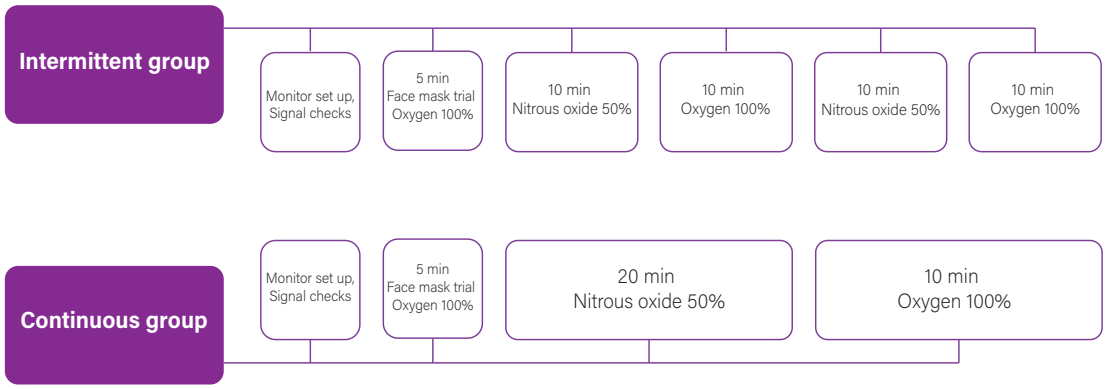


***Figure 3.1*** *Sub-anesthetic study protocol*

for each subject in MNE Python, hence creating continuous raw data for the entire recording period in all subjects' cases.

## 3.2 Pre-processing of raw EEG

Data pre-processing is required before any useful data analysis can be done on the acquired data. However, it is often difficult to choose the best processing pipeline due to the lack of a gold standard. The pre-processing pipeline implemented used the MNE-python package. MNE-python is an open-source package for the exploration, visualization, and analysis of human neurophysiological data such as EEG, magnetoencephalography (MEG), stereo EEG, intracranial EEG, near-infrared spectroscopy, and more in the Python environment. The pipeline was implemented in two main steps. First in the structuring and alignment of the raw EEG data. It involved the concatenation of unique subjects' data, renaming the files to commonly used names, dropping of non-relevant channels, assigning channel types to electrode signals and setting individual subject montages. The second stage processed these structured data to clean data. Filtering between (0.1 Hz to 40 Hz) was done to remove undesired frequency components of the signal, and also there was division into trials (epochs) of non-overlapping 30 seconds windows. The auto-reject algorithm was implemented to reject bad trials and repair bad sensors in the EEG signal. We applied the independent component analyses (ICA) technique next to remove prevalent artefact components scoring more than 0.5 and finally the auto-reject algorithm was implemented again to produce clean EEG data.

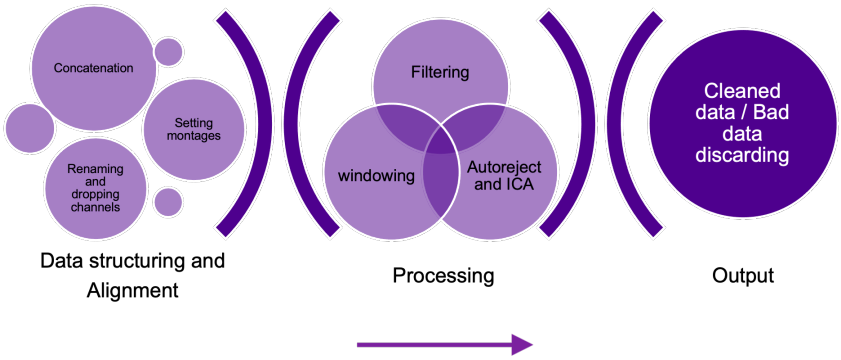


***Figure** 3.2 Implemented EEG pre-processing pipeline*

### 3.2.1 Cluster computing

Implementing the pre-processing pipeline stated above for all the subjects would take a significant amount of time to be completed on a local PC. A better alternative was to use clustered computers to execute the tasks. The idea behind cluster computing is to bring together several computers that can be closely or loosely connected in order to act as one entity. As a result, it appears that there is one system since all the computers are connected and performing the same operations. A cluster computer consists of cluster nodes, cluster operating system, the node or switch interconnect and lastly the network switching hardware. The Narvi is Tampere University's high-performing computing SLURM cluster. it consists of 140 CPU-only nodes with 3000+ CPU cores. Narvi also has 22 nodes with different GPU nodes with 4 GPUs in each. This makeup makes it useful for researchers, faculty members and students at the university. The processing of the raw EEG files was completed within an hour.

### 3.2.2 Autoreject and ICA

Autoreject is a library that automatically rejects and repairs bad trials in both magneto- and electro- encephalography (MEEG) signals. It combines cross-validation and robust evaluation measures to estimate the optimal peak-to-peak threshold used in identifying bad trials in MEEG [56].

ICA – Independent component analysis is an algorithm that separates mixed signals according to their sources. That is, it localizes independent signals that have been mixed. In MEEG, ICA could decompose artifactual signals into several components so that components resembling non-brain signals can be removed from the signal before reconstruction. The Autoreject technique was applied to the EEG signal

trials before and after ICA. Bad trials were removed before the computation of signal source localization on non-artifactual signals. During this process, a threshold of 0.5 was set to exclude blink artefact components from the signal. A new signal was reconstructed using the ICA parameter applied to the copy of the original EEG trial data. Autoreject was applied the second time on the resulting signal to reject and repair signal trials.

### 3.2.3 Filtered signal segmentation

To effectively analyse the connectivity properties of the filtered signals at the various conditions of the experiment, some python functions were written. They include getting the actual time stamps comprising of epochs within the specified conditions. This was possible because the time stamps for all the subjects were collated into a single excel file. A function reads the time values and converts them into the equivalent seconds of when the anaesthetic is on and off for the continuous cases and multiple on-and-off states for the intermittent cases. These values were then used in other functions to read the filtered signal and appropriate epochs corresponding to before, during and after the introduction of nitrous oxide for each of the subjects. Hence, this splits the data of each subject into a number of conditions. It was now possible to compute the spectral connectivity of these conditions in all the cases.

## 3.3 Implementation of wPLI

The Weighted Phase Lag Index, a new member of the phase-synchronization family was initiated to increase the capability of detecting true phase-synchronization changes, to reduce noise source effects, and to reduce the influence of phase changes of the coherence based on the imaginary component of the cross-spectrum [10]. These attributes make wPLI a suitable tool for graph analysis, as it has a more robust relationship with true phase consistency [57]. The EEG sensors could be considered as nodes and the wPLI values between sensors as links between the nodes in a graph network. In this work, the spectral connectivity across the trials was computed using this method for each subject. A connectivity matrix comprising all the electrode pair values was realised for each subject for each segmentation. The matrix values represent the connectivity strength between two EEG channels, and these values have also been represented in circular connectivity graphs, as shown in the next chapter of this work.

## 3.4 Statistical Analysis

The significance levels for this analysis were set at the 5% (i.e. $\alpha = 0.05$) level using student t-tests before beginning the analysis.

### 3.4.1 Surrogate dataset

An inter-subject EEG surrogate test was done to determine a null distribution for significance tests using surrogate data. This test assumes independence between EEG signals from different subjects. Despite the fact that the properties of EEG signals from one subject may not match those of another subject when viewed through the lens of surrogate data, inter-subject EEG signal pairs (two EEG signals from different subjects) were treated as surrogates for intrasubject EEG signal pairs (two EEG signals from the same subject)[58]. This is for two reasons: i) EEG signals are natural, not artificially generated, and ii) inter-subject EEG signals do not exhibit interdependence, which is often examined in intrasubject EEG signals. 19 EEG channels were randomly selected and the wPLIs were calculated for each pair that did not belong to the same subject to create surrogate datasets. These surrogate datasets were therefore assumed to preserve properties of before, during or after subanaesthetic EEG connectivity of the original data. Therefore, a significance test to determine if the original data has these randomized properties can be performed [58].

Scipy's statistical function was used to extract the p-values of these randomly selected intra-subject channel pairs. A null distribution of connectivity values was generated for each phase and frequency band of the experiment. Considerations of the continuous and intermittent cases were observed, thus, multiple distributions of surrogate datasets were retrieved. Furthermore, each subject's connectivity results in the specified categories were compared with a corresponding surrogate dataset to get the p-values.

### 3.4.2 Significance of connectivity across phases

To significantly ascertain the phase changes before, during and after the Nitrous oxide was introduced, EEG connectivity was computed and compared across the phases. This approach like the surrogate test above considered each band of EEG in the analysis for both continuous and intermittent cases. P-values were retrieved for each subject in a table.

### 3.4.3 Hypothesis testing

Hypothesis testing in EEG connectivity is a statistical method used to determine the significance of a relationship between two or more EEG signals. It involves formulating a hypothesis about the presence or absence of a connectivity relationship, collecting EEG data, and comparing the observed connectivity relationship to what would be expected by chance using statistical tests. The goal of hypothesis testing is

to determine whether the observed relationship is statistically significant, meaning that it is unlikely to have occurred by chance and provides evidence to support the hypothesis. If the relationship is statistically significant, it suggests that the signals are connected and that changes in one signal are likely to be related to changes in the other signal.

A hypothesis test was carried out to determine if the p-values obtained were statistically significant so as to inform how the surrogate dataset generated from inter-subject EEG pairs corresponds to the original dataset. Secondly, another hypothesis conducted was to check the statistical significance among experiment phases of each subject. The results will indicate the extent to which nitrous oxide-induced changes in EEG connectivity.

# 4 Results

An overview of the outcomes of the activities described in the methodology is presented in this section. Graphs and tables are presented summarizing the results of the EEG pre-processing, connectivity computations, hypothesis test and p-values obtained for each subject in the continuous and intermittent experiment groups. All graphs were plotted with MNE Python, and the tables containing p-values for each case were also collected from a Python dictionary variable output. Although only two samples of subjects' circular graph are shown in this section, all other graphs plots for every subject is shown in Appendix A. The overall results are summarized in this section.

## 4.1 EEG Pre-processing

This section describes the state of the raw data and outcomes of the pre-processing pipeline implemented. After concatenating the unique subject's raw data, Figure 4.1 shows all the data plotted with respect to the duration of the experiment. Subjects were renamed to fit the pre-processing pipeline and for effective analysis of the experimental phases, their time stamps were extracted as shown in Table 4.1. Both the table and the raw plot indicate that six of the subjects had incomplete experimental phases. The total number of subjects that could be analysed was reduced to 14 out of 20. However, all of the data collected passed through the pre-processing pipeline.

There are a couple of several eyes blinks and movement artefacts in Figure 4.3(a) and 4.3(c). Typically, eye blink artefacts are ten times larger than ongoing EEG, which is why they are so problematic. It should be noted that only five trials are shown in the images in order to clearly display these artefacts. Eye blink artefacts are picked up the strongest by the frontal electrodes Fp1 and Fp2 and other electrodes with labels starting with "F" [59]. These artefacts show a sharp increase and decrease in electrical potential, and an inversion of the artefact at more posterior electrodes, such as TP9 and TP10. The ICA component ICA000 can be used to identify these artefacts as independent sources shown in 4.2(a) and attenuate them by zeroing the component.

On the other hand, constant eye positions don't affect EEG recordings as the dipole created by the retina is constant. Nevertheless, when the eyes move to observe different locations in space, the dipole created by the retina moves and the electrodes on the scalp detect this movement, leading to changes in electrical potential at frontal electrodes on one side of the head and the opposite change on the other side. The

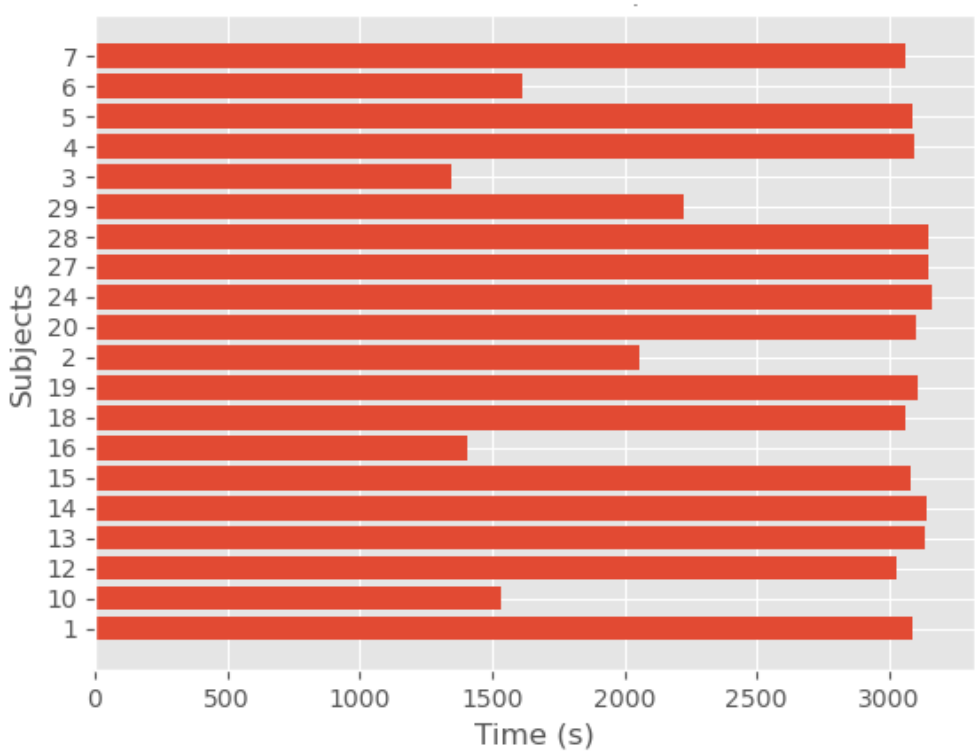


***Figure 4.1*** *Plot of subjects indicating the duration of examination before pre-processing of the data*

horizontal eye movement roughly generates a ”square wave” effect at electrodes F7 and F8, with F7/F3 becoming positive and F8/F4 becoming negative [59]. These artefacts are identified because the polarity magnitude at F7 and F8 is the same but in different directions. The ICA decomposition of this eye movement shows as bilateral frontal topography in Figure 4.2(b). It was possible to remove these artefactual sources in the pre-processing pipeline.

Overall, there were 9 successfully cleaned EEG signals; 5 from the continuous group and 4 from the intermittent group.

## 4.2 EEG Connectivity graphs

EEG connectivity refers to the correlation of EEG signals between different brain regions. It is a measure of how electrical signals in the brain are synchronized across different locations, reflecting the communication and coordination between different brain regions. Examples of the EEG connectivity results are shown in the circular graphs for both continuous and intermittent cases. Inhaling the sub-anaesthetic caused several changes to occur. Instead of showing the connectivity strength among all the pairs of electrodes, the 12 electrode pairs with the strongest connectivity

***Table 4.1*** *Raw data with time stamps*

| subject | renamed | start | gas_on | gas_off | gas_on2 | gas_off2 | end | total |
|---|---|---|---|---|---|---|---|---|
| 1 | 1 | 12:56:46 | 13:07:21 | 13:27:09 | | | 13:48:12 | 0:51:26 |
| 2 | 2 | 14:19:24 | 14:30:07 | 14:33:08 | | | 14:54:01 | 0:34:37* |
| 3 | 3 | 14:01:30 | 14:10:22 | 14:12:15 | | | 14:23:20 | 0:21:50* |
| 4 | 4 | 13:56:57 | 14:08:15 | 14:28:18 | | | 14:48 | 0:51:04 |
| 5 | 5 | 13:34:18 | 13:46:08 | 13:56:09 | 14:06:08 | 14:16:06 | 14:26:23 | 0:52:05 |
| 6 | 6 | 12:08:36 | 12:19:12 | 12:22:46 | | | 12:25:00 | 0:16:24* |
| 7 | 7 | 8:42:31 | 8:55:07 | 9:14:23 | | | 9:35:25 | 0:52:54 |
| 28 | 8 | 8:30:29 | 8:43:09 | 9:03:08 | | | 9:23:24 | 0:52:55 |
| 29 | 9 | 15:47:16 | 15:58:16 | 16:14:23 | | | 16:24:36 | 0:37:20* |
| 10 | 10 | 9:09:54 | 9:22:07 | 9:25:01 | 9:25:22 | | 9:35:34 | 0:25:40* |
| 24 | 11 | 12:28:05 | 12:40:06 | 13:00:07 | | | 13:20:18 | 0:52:13 |
| 12 | 12 | 13:36:46 | 13:47:08 | 13:57:09 | 14:07:07 | 14:17:07 | 14:27:25 | 0:50:39 |
| 13 | 13 | 12:12:18 | 12:24:42 | 12:34:32 | 12:44:24 | 12:54:24 | 13:04:44 | 0:52:26 |
| 14 | 14 | 10:26:23 | 10:36:17 | 10:45:32 | 10:55:08 | 11:05:07 | 11:15:24 | 0:49:01 |
| 15 | 15 | 12:38:27 | 12:51:50 | 13:01:30 | 13:11:07 | 13:21:06 | 13:31:28 | 0:53:01 |
| 16 | 16 | 8:29:46 | 8:40:07 | 8:43:45 | | | 8:45:00 | 0:15:14* |
| 27 | 17 | 13:54:42 | 14:07:49 | 14:17:23 | 14:27:17 | 14:37:05 | 14:47:20 | 0:52:38 |
| 18 | 18 | 14:02:18 | 14:13:07 | 14:23:09 | 14:33:10 | 14:43:11 | 14:53:29 | 0:51:11 |
| 19 | 19 | 12:41:01 | 12:52:11 | 13:12:26 | | | 13:33:17 | 0:52:16 |
| 20 | 20 | 14:10:15 | 14:21:17 | 14:41:42 | | | 15:02:15 | 0:52:00 |

* Incomplete experiment

were plotted. This clearly identifies where or whether there are significant changes in connectivity strength among the electrode pairs in the various conditions.

**Subject 1** is a member of the continuous group and its circular connectivity graphs is shown in Figure 4.4, 4.5, 4.6, 4.7.

The images depict changes in neuronal electrode pairs in the given frequency range and their connectivity strength before, during, and after anaesthesia.

In the next set of circular graphs Figure 4.8, 4.9, 4.10, 4.11, we find those of subject 12, part of the intermittent group.

## 4.3 P-values - Continuous vs Intermittent cases

### 4.3.1 Surrogate analysis

Among the continuous group, the original data distribution was found to be statistically significant when compared to the surrogate data in most instances. In Table 4.2 the theta band recorded the highest significant difference as shown in every phase of the experiment (before, during and after anaesthesia). The alpha band had

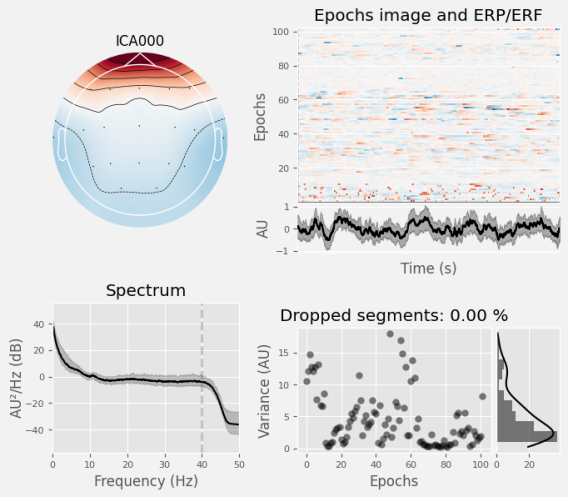


(a) Frontal Topography

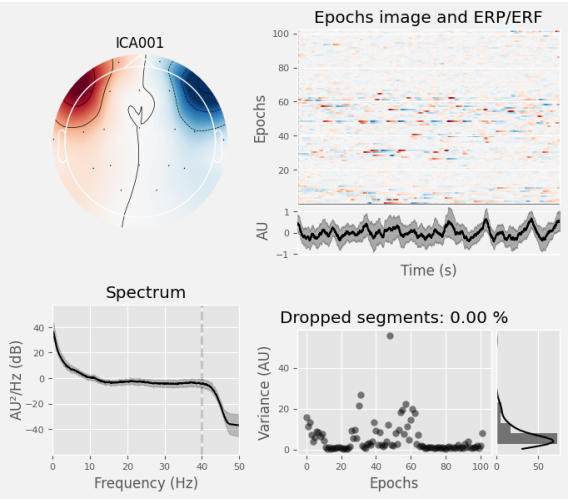


(b) Frontal bilateral topography

***Figure 4.2*** *ICA components indicating eye blink and eye movement artefacts independent sources that are zeroed during pre-processing*

the least significant difference which is seen across 3 subjects with 4 non-significant p-values instances. During the nitrous oxide application phase, the delta band p-values observed are non-significant in 2 of the subjects. In the beta band, 3 out of 4 of the subjects' results were significant.

In the intermittent group, most of the results are also statistically different from the surrogate data generated. However, the theta band recorded some statistically non-significant results compared to the continuous case. The alpha and theta bands had the most statistically significant results across the 5 phases of the experiment *before, during1, after1, during2, after2*. The band with the least connectivity p-values among the subjects is the beta band, where in 7 instances, values among all

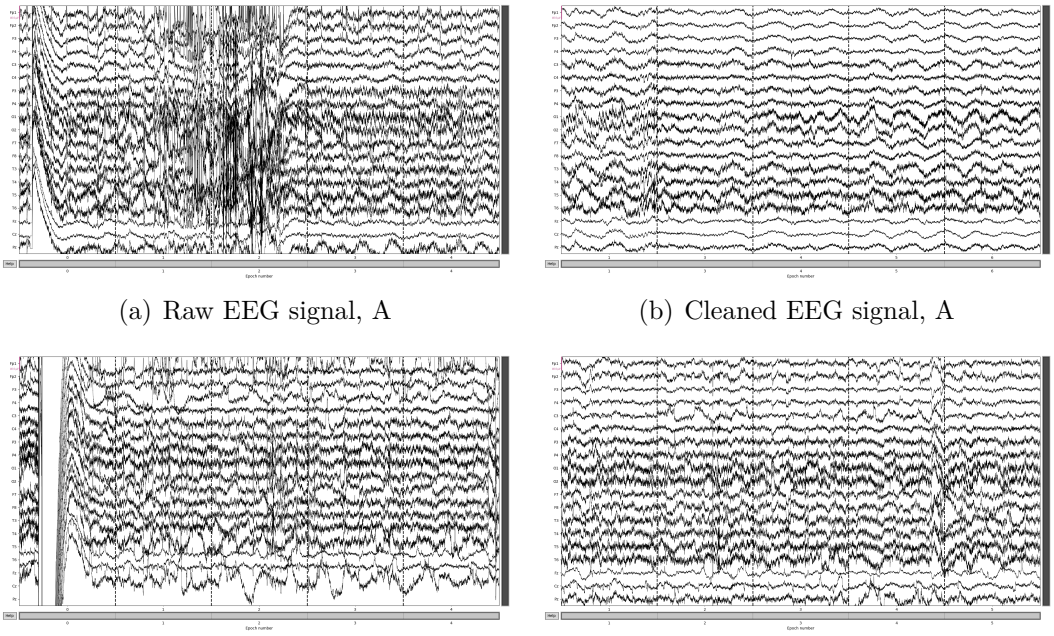

(a) Raw EEG signal, A

(b) Cleaned EEG signal, A

(c) Raw EEG signal, B

(d) Cleaned EEG signal, B

***Figure 4.3*** *Instances of EEG pre-processing results: raw signals (left), clean signals (right)*

the subject experimental phases are not statistically significant.
Based on the results in the tables, the beta band offers the least statistically significant p-values in the surrogate test for intermittent groups. It contrasts the result of the continuous group surrogate test where the beta band had just two instances of statistical non-significance on one subject.

### 4.3.2 Across experimental phases

It was necessary to measure how the phase processes of the experiment vary from each other for all the subjects individually. This compares the continuous and intermittent conditions to know where the most significant changes occurred and which frequency band are these changes most significant. The Tables 4.4 and 4.5 show the resulting p-values across experimental phases for each subject.

#### Continuous group individual analysis

The continuous group had 3 experimental phases i.e. the *before, during* and *after* anaesthesia was administered to the subjects. Since the aim of this work is to investigate the effect of nitrous oxide after was induced in the subjects, therefore, we compared the *before vs after* phases results for each of these subjects as shown in Table 4.4.

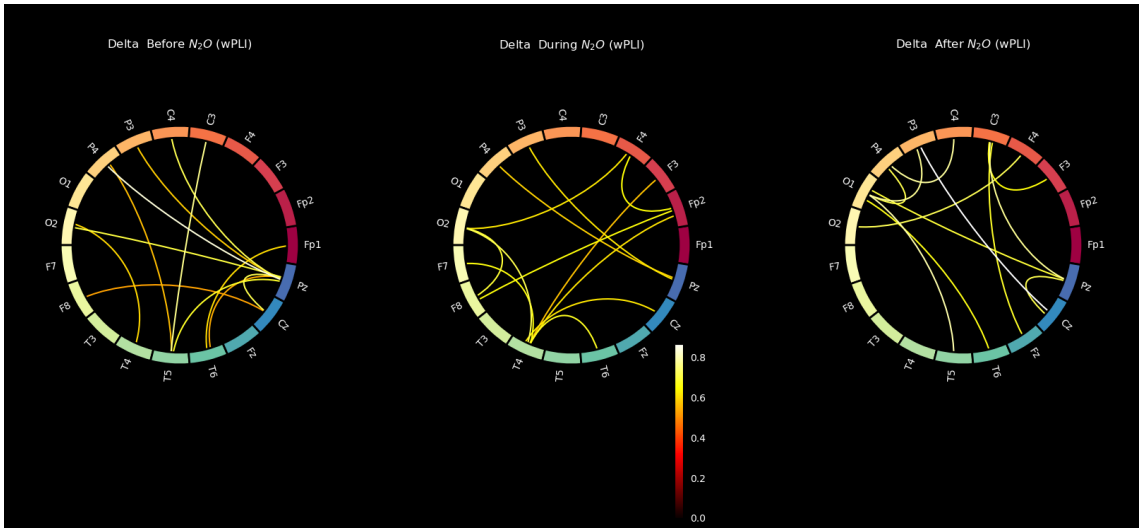


***Figure 4.4*** *Circular connectivity graph of subject 1 in the delta band showing the 12 strongest connectivity strengths between pairs of electrodes in episodes of before, during and after nitrous oxide anaesthesia.*

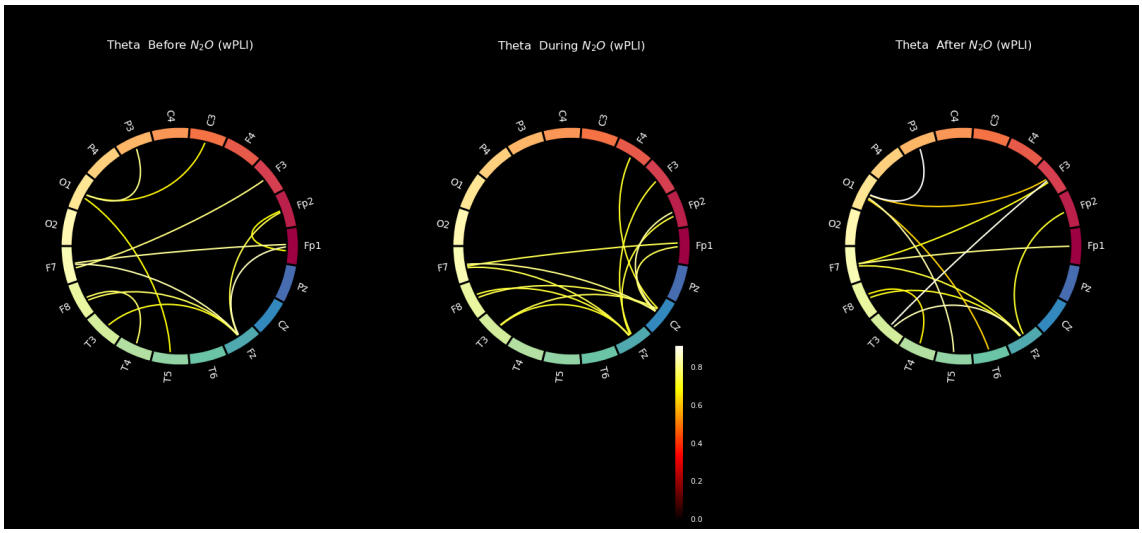


***Figure 4.5*** *Circular connectivity graph of subject 1 in the theta band showing the 12 strongest connectivity strengths between pairs of electrodes in episodes of before, during and after nitrous oxide anaesthesia.*

**Subject 1**: Both alpha and beta band comparison of *before vs after* results are statistically significant. Whereas the results recorded in the delta and theta bands were found to be non-significant statistically.

**Subject 4**: There are significantly varying connectivity properties of EEG in theta, alpha and beta band while only the delta band contained statistically non-significant results when the state of connectivity was compared for *before vs after* phases.

**Subject 7**: The results computed for *before vs after* phases across the 4 frequency bands were statistically significant in two out of the four frequency bands. This is

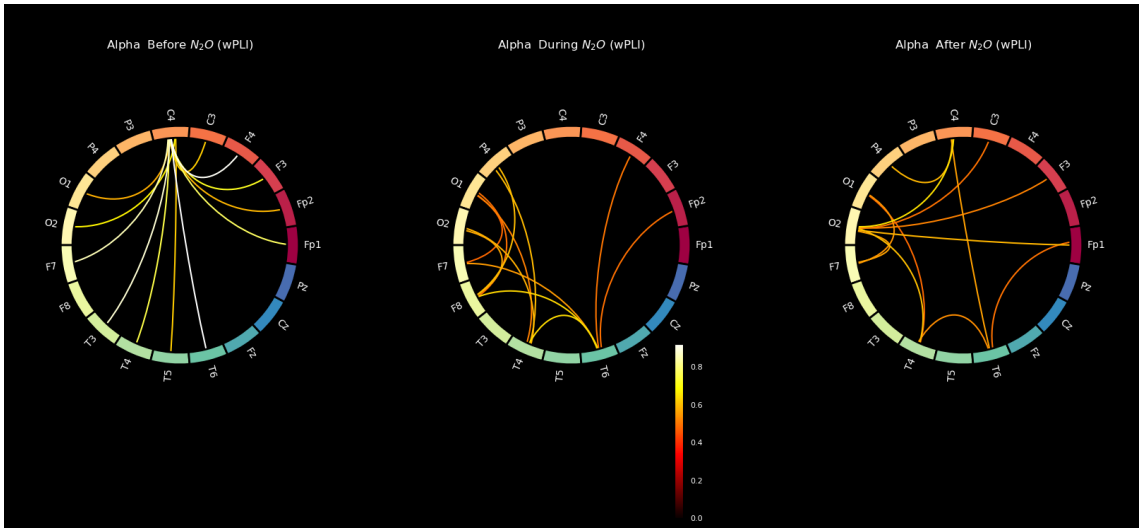


***Figure 4.6*** *Circular connectivity graph of subject 1 in the alpha band showing the 12 strongest connectivity strengths between pairs of electrodes in episodes of before, during and after nitrous oxide anaesthesia.*

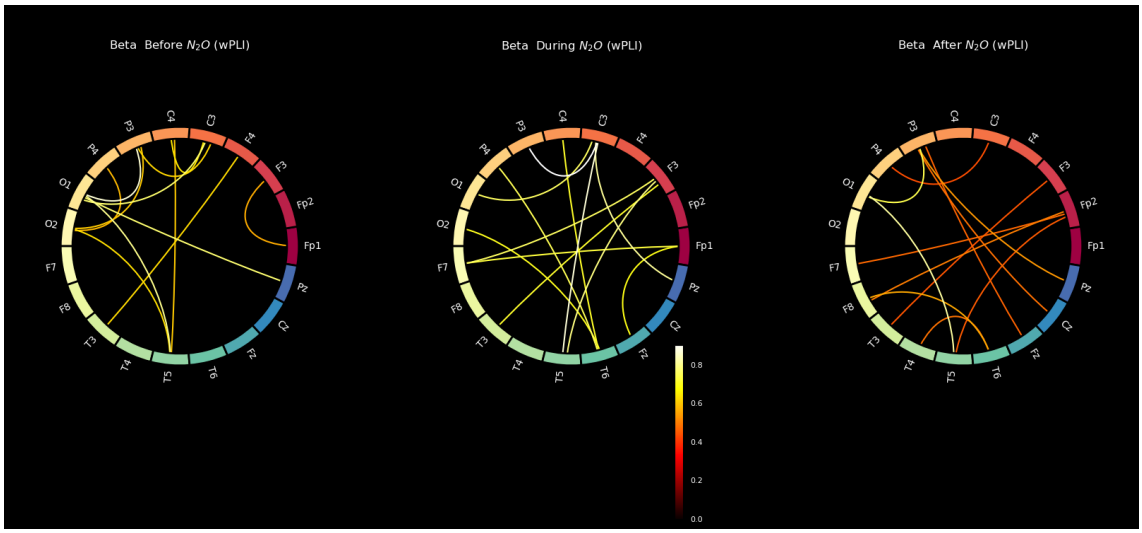


***Figure 4.7*** *Circular connectivity graph of subject 1 in the beta band showing the 12 strongest connectivity strengths between pairs of electrodes in episodes of before, during and after nitrous oxide anaesthesia.*

in the alpha and beta bands while the delta and theta bands are not statistically significant.

**Subject 11**: Three out of the four frequency bands were statistically significant when connectivity was computed for *before vs after* phases. These include the theta, alpha and beta bands while the delta band is not significant as shown in the table.

**Subject 19**: This subject had all statistically significant in all the bands when the *before vs after* phases were computed. It is clear across all EEG frequency bands that there is a significant difference between the phases.

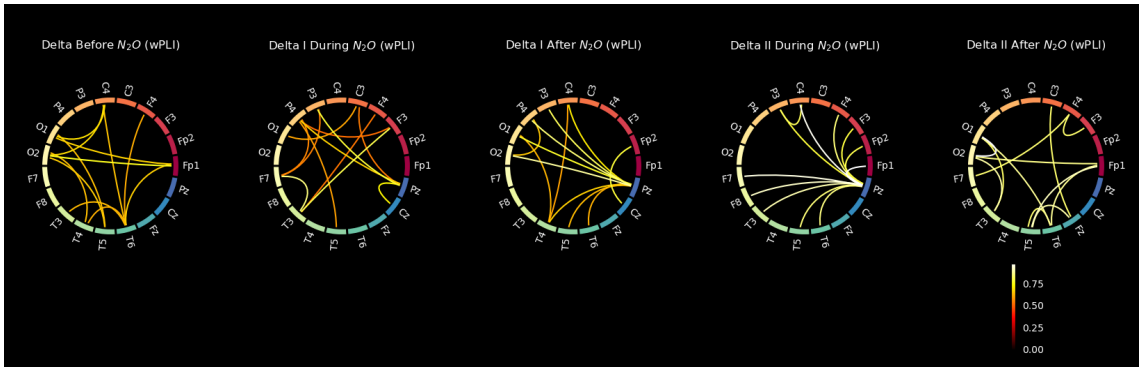


***Figure 4.8*** *Circular connectivity graph of subject 12 in the delta band showing the 12 strongest connectivity strengths between pairs of electrodes in episodes of before, during1, after1, during2 and after2 nitrous oxide anaesthesia.*

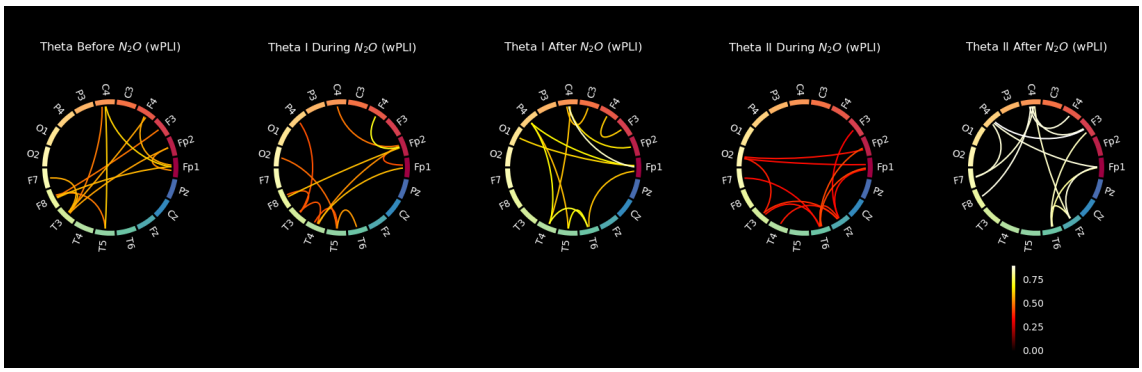


***Figure 4.9*** *Circular connectivity graph of subject 12 in the theta band showing the 12 strongest connectivity strengths between pairs of electrodes in episodes of before, during1, after1, during2 and after2 nitrous oxide anaesthesia.*

The results among the continuous group show that the lower frequency bands were the least affected in connectivity after the introduction of nitrous oxide. In four out of five instances, the result was not statistically significant in the delta band. In two out of five, the theta band showed no significant variation. Beta and alpha are the bands most affected by this phenomenon, as every result is statistically significant.

### Intermittent group individual analysis

The intermittent group had 5 phases (*before, during1, after1, during2 and after2*) of the experiment. We however compared the before nitrous oxide and the after phases of nitrous oxide introduction and also the after1 and after2 phases to have a clearer understanding of the effect of the anaesthesia and how these changes differ from each other in the intermittent case. The result is shown in Table 4.5.

**Subject 12**: In *before vs after1* comparison, the p-value was found to have a statistically significant result all through the alpha band. However, the results computed

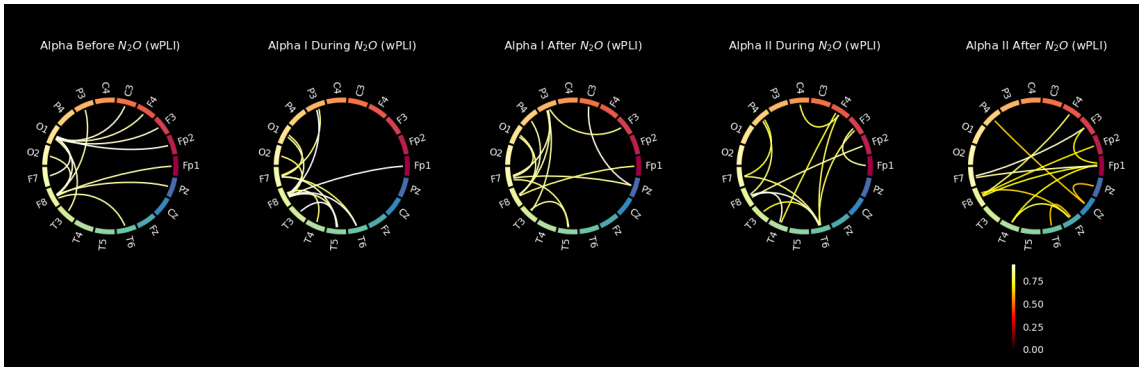


***Figure 4.10*** *Circular connectivity graph of subject 12 in the alpha band showing the 12 strongest connectivity strengths between pairs of electrodes in episodes of before, during1, after1, during2 and after2 nitrous oxide anaesthesia.*

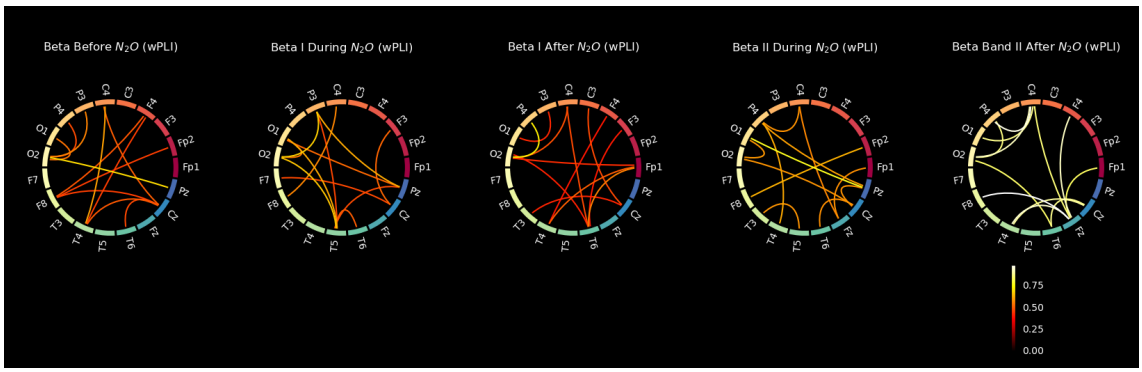


***Figure 4.11*** *Circular connectivity graph of subject 12 in the beta band showing the 12 strongest connectivity strengths between pairs of electrodes in episodes of before, during1, after1, during2 and after2 nitrous oxide anaesthesia.*

for *before vs after2* and *after1 vs after2* are statistically significant in all the frequency bands.

**Subject 13**: In this subject, the EEG connectivity values for the phases are shown to vary significantly in both delta and alpha bands. Two each in theta and beta band p-values are statistically significant in both *before_vs_after2* and *after1_vs_after2*. Based on this, there is no significant difference between the pre-anaesthesia phase and the first post-anaesthesia phase in the theta and beta bands.

**Subject 14**: Among the three instances, the highest non-significant p-values were observed in the theta band. The p-values for the delta and alpha bands were statistically non-significant once in each. The beta band had two instances where the p-values were not significant. Aside from these, all other results are statistically significant.

**Subject 18**: The results, in this case, were somewhat statistically significant. All the delta band instances were significant, whereas the theta, alpha and beta bands had a single occurrence of non-statistical significant results.

***Table 4.2*** *Continuous group surrogate analyses - p_values*

| | delta | theta | alpha | beta |
|---|---|---|---|---|
| Subject 1 | | | | |
| before | NS | ** | ** | NS |
| during | * | *** | ** | *** |
| after | *** | *** | * | NS |
| Subject 4 | | | | |
| before | * | *** | NS | *** |
| during | *** | *** | *** | *** |
| after | *** | *** | NS | *** |
| Subject 7 | | | | |
| before | * | *** | NS | *** |
| during | *** | *** | ** | *** |
| after | *** | *** | *** | *** |
| Subject 11 | | | | |
| before | *** | *** | *** | *** |
| during | NS | *** | *** | *** |
| after | *** | *** | *** | *** |
| Subject 19 | | | | |
| before | ** | *** | *** | *** |
| during | NS | ** | NS | *** |
| after | *** | *** | *** | *** |

NS - Not Significant
Significant * 0.005 - 0.05, ** 0.00005 - 0.005, *** 0 - 0.00005

Overall the intermittent cases, the most affected EEG frequency bands in post-anaesthesia comparison are the delta and alpha bands. The theta band is the least affected, followed by the beta band. This result is in contrast with the results gathered from the continuous group, where higher frequency bands generated most of the statistically significant results.

***Table 4.3*** *Intermittent group surrogate analyses - p_values*

| | delta | theta | alpha | beta |
|---|---|---|---|---|
| Subject 12 | | | | |
| before | * | * | *** | *** |
| during1 | * | *** | *** | NS |
| after1 | *** | ** | *** | *** |
| during2 | *** | *** | *** | * |
| after2 | *** | *** | *** | ** |
| Subject 13 | | | | |
| before | *** | *** | ** | * |
| during1 | *** | NS | ** | *** |
| after1 | *** | NS | *** | NS |
| during2 | *** | * | *** | *** |
| after2 | * | NS | *** | *** |
| Subject 14 | | | | |
| before | *** | NS | *** | NS |
| during1 | *** | *** | *** | NS |
| after1 | *** | NS | *** | *** |
| during2 | *** | *** | *** | ** |
| after2 | ** | *** | *** | NS |
| Subject 18 | | | | |
| before | *** | *** | * | NS |
| during1 | ** | *** | *** | NS |
| after1 | ** | *** | * | *** |
| during2 | NS | *** | NS | * |
| after2 | *** | *** | * | *** |

NS - Not Significant
Significant * 0.005 - 0.05, ** 0.00005 - 0.005, *** 0 - 0.00005

***Table 4.4*** *Continuous group p-values showing the comparison of before vs after anaesthesia*

| | delta | theta | alpha | beta |
|---|---|---|---|---|
| Subject 1 | | | | |
| before_vs_after | NS | NS | * | * |
| Subject 4 | | | | |
| before_vs_after | NS | ** | * | ** |
| Subject 7 | | | | |
| before_vs_after | NS | NS | *** | *** |
| Subject 11 | | | | |
| before_vs_after | NS | *** | * | *** |
| Subject 19 | | | | |
| before_vs_after | *** | *** | * | *** |

NS - Not Significant
Significant * 0.005 - 0.05, ** 0.00005 - 0.005, *** 0 - 0.00005

***Table 4.5*** *Intermittent group p-values showing the comparison of before vs after anaesthesia*

| | delta | theta | alpha | beta |
|---|---|---|---|---|
| Subject 12 | | | | |
| before_vs_after1 | NS | NS | ** | NS |
| before_vs_after2 | *** | *** | *** | *** |
| after1_vs_after2 | *** | *** | *** | *** |
| Subject 13 | | | | |
| before_vs_after1 | *** | NS | * | NS |
| before_vs_after2 | ** | *** | *** | *** |
| after1_vs_after2 | ** | *** | *** | *** |
| Subject 14 | | | | |
| before_vs_after1 | NS | NS | *** | NS |
| before_vs_after2 | ** | NS | *** | * |
| after1_vs_after2 | ** | NS | NS | NS |
| Subject 18 | | | | |
| before_vs_after1 | ** | *** | NS | *** |
| before_vs_after2 | *** | NS | *** | NS |
| after1_vs_after2 | *** | *** | * | *** |

NS - Not Significant
Significant * 0.005 - 0.05, ** 0.00005 - 0.005, *** 0 - 0.00005

# 5 Discussion

This study provides insight into how to monitor the brain state and consciousness of subjects for major depression studies by examining the effect of nitrous oxide on brain connectivity. It aimed to substantiate the scientific understanding of how and to what extent the cortical unit interactions are affected by the possible depression-alleviating agent nitrous oxide. Having assessed both the benefits and caveats of the various EEG connectivity metrics, the wPLI technique of phase synchronization was applied. In the following paragraphs, the results will be discussed along with their interpretation, implications, limitation of the study and suggestions for further research.

Analyses have shown that nitrous oxide alters brain connectivity on a variety of levels. Indications in the graph plots showed that raw EEG data were suitably pre-processed and eliminated a considerable amount of signal noise arising from eye blinks so the nitrous oxide effect could be assessed reliably. Nevertheless, some EEG data quality was poor such that their correction was ineffective in the pre-processing pipeline. Changes in neuronal interactions were consistent with the introduction of nitrous oxide. The strength of these changes differs among the subjects and frequency bands considered. In the surrogate test, the significance level indicates that the wPLIs of original intra-subject EEG signals are not correlated. Post-anaesthesia, higher frequency bands of EEG were mostly affected by prolonged gas exposure, while beta waves were least affected by intermittent gas exposure.

It is hypothesized that phase changes in neuronal synchronization serve as mechanisms for neuronal communication. The results of the surrogate test suggest that the data generated can provide an appropriate significance test. The results presented by wPLI are consistent with the graph analysis study on the nitrous oxide sedative effect [9]. However, the phase synchronization metric deployed in this study determined whether there is oscillatory synchrony between brain regions at similar frequency ranges in pre and post-conditions of anaesthesia. In the continuous group, the EEG connectivity dynamics acquired indicate strict variation in beta and alpha waves wPLI distribution of the pre and post-anaesthesia. This contrasts the results acquired in the intermittent gas exposure group where the beta band recorded the minimum change among the four frequency ranges. Since major depression disorder has been associated with alterations in mood, cognitive ability, sensorimotor functions and homeostatic functions [60], the data, therefore, suggest that continuous nitrous oxide exposure may be a more effective therapy protocol if found to be a suitable antidepressant. The reason is that most of the stated depression characteristics

are more associated with beta frequency. In addition, [48] found delta oscillations to be induced by nitrous oxide using power spectral density (PSD). Although results from PSD and network analysis performed on functional correlation (FC) shows some strong relation, PLI vs PSD comparison is not as straightforward as PLV vs PSD [61]. However, it suggests that PSD and FC results may not be independent and should not be separated. Instead, they should be analyzed together to provide a more comprehensive view of the result. Considering this, it would seem that the wPLI technique cannot easily confirm the induced delta oscillation. Nonetheless, the unvarying delta distribution in the continuous group may imply increased delta wave activities in synchrony between neuronal pairs of EEG electrodes. In another study [62], depression disorder was found to not be associated with the delta band but with theta, alpha and beta bands of EEG electrophysiology properties. The intermittent group result showed more variation in both delta and alpha EEG bands.

This study has some potential limitations. It is difficult to make major inferences on the effects of nitrous oxide due to the low number of subjects, few data collected, sensor-level analysis and the lack of sufficient prior research on the topic. Five and four subjects from the continuous and intermittent groups respectively are insufficient to draw general conclusions. The sample size is too small to make group analyses that identify the significant relationships in the data and this is why a case-by-case analysis has been applied in this work. Recruiting more subjects and collecting multiple data after anaesthesia treatment can be considered for future research. Nitrous oxide had been identified to alleviate symptoms of depression in some subjects by [8]. The study investigated the changes on the 21-item Hamilton Depression Rating Scale resulting from nitrous oxide treatment 2hrs and 24hrs after the treatment. The assessment of neuronal connectivity just after the treatment was necessary, however, additional data collection after 2hr and 24hr can be helpful to establish a better understanding of the neuronal circuit mechanism of nitrous oxide and relate it with the referenced study. It is imperative to note the following considerations when analyzing at the sensor level: EEG channels do not necessarily correlate with the source location [63]; however, this study assumes so, and despite the application of the wPLI method, spurious estimates of functional connectivity between the channels may still occur as a result of field spread and volume conduction [64, 65]. The other limitation observed in this study is because of insufficient previous studies on brain connectivity arising from the identified antidepressants. There is an obvious need to investigate other NMDA-R features in neuronal connectivity. It would provide insight into the common function of nitrous oxide with other NMDA -R in brain connectivity relating to anti-depression effects. Using source-level data to investigate the effect of nitrous oxide could also help to quantify the effects of nitrous oxide on brain interactions.

In summary, the wPLI method of phase synchronization was chosen after weighing the advantages and disadvantages of the different EEG connectivity measurements. The graph plots show that the raw EEG data was sufficiently pre-processed to remove eye blink noise and estimate the nitrous oxide effect. All of the subjects' neural interactions were consistently altered by nitrous oxide. These findings support the conclusions of [9]'s graph analysis study on the sedative effects of nitrous gas. Additionally, it was shown by [48] that nitrous oxide causes delta oscillations, and some participants in both groups displayed elevated delta connectivity values. According to one study [62], theta, alpha, and beta electrophysiological bands, rather than the delta band, were associated with depressive disorder. This study discovered that the beta band connection strength was noticeably diminished in the continuous group participants. Small data size, sensor-level data and insufficient prior research are potential limitations of this work. A general conclusion cannot be drawn since there is not enough research on how the antidepressants identified affect brain connections. More research into how nitrous oxide affects brain state and consciousness may be possible with the addition of more participants, several data points after nitrous oxide administration, and source-level data analysis.

# 6 Conclusions and Future perspective

This chapter serves as a conclusion, summarizing the primary research findings in relation to the research objectives, and highlighting their value and contribution. It is important to acknowledge the limitations identified in the preceding chapter, namely the relatively small sample size, which hindered the interpretation of the results and limited conclusions regarding complex phenomena. However, this section will provide a broader perspective on potential avenues for future research.

The primary objective of this investigation was to examine the impact of nitrous oxide on cortical interactions. This research was motivated by the need to expand our understanding of the claimed antidepressant effect of nitrous oxide, as reported by some studies. Based on the findings of this investigation, the following conclusion can be drawn.

- The results indicate that nitrous oxide alters information processed during anaesthesia, as observed on the EEG bands. The beta band connectivity was significantly reduced at prolonged gas exposure than at intermittent exposure, indicating a faster loss of consciousness in the former condition.
- This study does not, however, claim any major findings about how nitrous oxide can relieve depression. It is necessary to collect more data from a larger study of known antidepressants to establish nitrous oxide's baseline impact on depression symptoms relating to neural interactions.
- Future studies can benefit from the considerations made in this study. The wPLI connectivity metrics used after the pre-processing pipeline are more reliable due to the fact that they are less prone to noise caused by volume conduction. In addition, further research may consider other connectivity techniques that may be more suitable for any prior assumptions about its data. By adding more subjects to this study, it should become easier to analyze EEG connectivity properties on a broader scale based on the pre-processing pipeline generated from this study.
- In any given condition, the Python algorithms provide efficient case-by-case analysis, and this can easily be optimized to make a group analysis that establishes a baseline understanding of nitrous oxide's effect on neuronal circuit mechanisms.

Considering this, further research in this area could yield valuable insights into the mechanism of action of nitrous oxide and its potential therapeutic applications in treating depression.

# References


[1] Christian O'Reilly and Mayada Elsabbagh. "Intracranial recordings reveal ubiquitous in-phase and in-antiphase functional connectivity between homotopic brain regions in humans". In: (June 2020). DOI: 10.1101/2020.06.19.162065.

[2] Shiva Asadzadeh et al. "A systematic review of EEG source localization techniques and their applications on diagnosis of brain abnormalities". In: *Journal of Neuroscience Methods* 339 (2020), pp. 1–23. ISSN: 1872678X. DOI: 10.1016/j.jneumeth.2020.108740. arXiv: 1910.07980.

[3] Guido Nolte et al. "Identifying true brain interaction from EEG data using the imaginary part of coherency". In: *Clinical Neurophysiology* 115.10 (2004), pp. 2292–2307. ISSN: 1388-2457. DOI: https://doi.org/10.1016/j.clinph.2004.04.029. URL: https://www.sciencedirect.com/science/article/pii/S1388245704001993.

[4] Narayan P Subramaniyam. *Source Localization in the EEG*. 2018. URL: https://sapienlabs.org/source-localization-in-the-eeg/ (visited on 12/01/2021).

[5] J. Olesen et al. "The economic cost of brain disorders in Europe". In: *European Journal of Neurology* 19.1 (2012), pp. 155–162. DOI: https://doi.org/10.1111/j.1468-1331.2011.03590.x. eprint: https://onlinelibrary.wiley.com/doi/pdf/10.1111/j.1468-1331.2011.03590.x. URL: https://onlinelibrary.wiley.com/doi/abs/10.1111/j.1468-1331.2011.03590.x.

[6] Marije aan het Rot et al. "Ketamine for Depression: Where Do We Go from Here?" In: *Biological Psychiatry* 72.7 (2012). Novel Pharmacotherapies for Depression, pp. 537–547. ISSN: 0006-3223. DOI: https://doi.org/10.1016/j.biopsych.2012.05.003. URL: https://www.sciencedirect.com/science/article/pii/S0006322312004179.

[7] Robert M Berman et al. "Antidepressant effects of ketamine in depressed patients". In: *Biological Psychiatry* 47.4 (2000), pp. 351–354. ISSN: 0006-3223. DOI: https://doi.org/10.1016/S0006-3223(99)00230-9. URL: https://www.sciencedirect.com/science/article/pii/S0006322399002309.

[8] Peter Nagele et al. "Nitrous oxide for treatment-resistant major depression: A proof-of-concept trial". In: *Biological Psychiatry* 78 (1 2015), pp. 10–18. ISSN: 18732402. DOI: 10.1016/j.biopsych.2014.11.016.

[9] Ji Min Lee et al. “Analysis of brain connectivity during nitrous oxide sedation using graph theory”. In: *Scientific Reports* 10.1 (2020), pp. 1–11. ISSN: 20452322. DOI: 10.1038/s41598-020-59264-0.

[10] Martin Vinck et al. “An improved index of phase-synchronization for electrophysiological data in the presence of volume-conduction, noise and sample-size bias”. In: *NeuroImage* 55.4 (2011), pp. 1548–1565. ISSN: 10538119. DOI: 10.1016/j.neuroimage.2011.01.055. URL: http://dx.doi.org/10.1016/j.neuroimage.2011.01.055.

[11] Somer Nacy et al. “Controlling a Servo Motor Using EEG Signals from the Primary Motor Cortex”. In: *American Journal of Biomedical Engineering* 2016 (Oct. 2016), pp. 139–146. DOI: 10.5923/j.ajbe.20160605.02.

[12] Jahangir Moini and Pirouz Piran. “Chapter 6 - Cerebral cortex”. In: *Functional and Clinical Neuroanatomy*. Ed. by Jahangir Moini and Pirouz Piran. Academic Press, 2020, pp. 177–240. ISBN: 978-0-12-817424-1. DOI: https://doi.org/10.1016/B978-0-12-817424-1.00006-9. URL: https://www.sciencedirect.com/science/article/pii/B9780128174241000069.

[13] Gregory Tierney and Ciaran Simms. “A Biomechanical Assessment of Direct and Inertial Head Loading in Rugby Union”. PhD thesis. Sept. 2018.

[14] W.O. Tatum et al. *Handbook of EEG Interpretation*. Springer Demos Medic Series. Springer Publishing Company, 2008. ISBN: 9781933864112. URL: https://books.google.no/books?id=ZrlxaOU133AC.

[15] Andrea Biasiucci, Benedetta Franceschiello, and Micah M. Murray. “Electroencephalography”. In: *Current Biology* 29.3 (2019), R80–R85. ISSN: 0960-9822. DOI: https://doi.org/10.1016/j.cub.2018.11.052. URL: https://www.sciencedirect.com/science/article/pii/S0960982218315513.

[16] *The 10-20 System for EEG - TMSi*. 2022. URL: https://info.tmsi.com/blog/the-10-20-system-for-eeg (visited on 09/26/2022).

[17] Soraia M. Alarcão and Manuel José Fonseca. “Emotions Recognition Using EEG Signals: A Survey”. In: *IEEE Transactions on Affective Computing* 10 (2019), pp. 374–393.

[18] Mahsa Soufineyestani, Dale Dowling, and Arshia Khan. “Electroencephalography (EEG) Technology Applications and Available Devices”. In: *Applied Sciences* 10.21 (2020). ISSN: 2076-3417. DOI: 10.3390/app10217453. URL: https://www.mdpi.com/2076-3417/10/21/7453.

[19] Christoph Guger, Brendan Allison, and Natalie Mrachacz-Kersting. *Brain-Computer Interface Research: A State-of-the-Art Summary 7, 2017*. July 2017, pp. 1–9. ISBN: 978-3-030-05667-4. DOI: 10.1007/978-3-030-05668-1_1.

[20] G. Schalk et al. “BCI2000: a general-purpose brain-computer interface (BCI) system”. In: *IEEE Transactions on Biomedical Engineering* 51.6 (2004), pp. 1034–1043. DOI: 10.1109/TBME.2004.827072.

[21] Christoph Guger, Theresa Vaughan, and Brendan Allison. *Brain-Computer Interface Research: A State-of-the-Art Summary 3, 2013*. Jan. 2013. ISBN: 978-3-319-09978-1. DOI: 10.1007/978-3-319-09979-8.

[22] Francisco Velasco-Álvarez, Álvaro Fernández-Rodríguez, and Ricardo Ron-Angevin. “Home Automation System Controlled Through Brain Activity”. In: *Computers Helping People with Special Needs: 18th International Conference, ICCHP-AAATE 2022, Lecco, Italy, July 11–15, 2022, Proceedings, Part II*. Milan, Italy: Springer-Verlag, 2022, pp. 105–112. ISBN: 978-3-031-08644-1. DOI: 10.1007/978-3-031-08645-8_13. URL: https://doi.org/10.1007/978-3-031-08645-8_13.

[23] Peining Pan, Gary Tan, and Aung Aung Phyo Wai. *Evaluation of Consumer-Grade EEG Headsets for BCI Drone Control - A*STAR OAR*. 2017. URL: https://oar.a-star.edu.sg/communities-collections/articles/13648 (visited on 09/28/2022).

[24] Daniel Cernea et al. “Controlling In-Vehicle Systems with a Commercial EEG Headset: Performance and Cognitive Load”. In: *Visualization of Large and Unstructured Data Sets: Applications in Geospatial Planning, Modeling and Engineering - Proceedings of IRTG 1131 Workshop 2011*. Ed. by Christoph Garth, Ariane Middel, and Hans Hagen. Vol. 27. OpenAccess Series in Informatics (OASIcs). Dagstuhl, Germany: Schloss Dagstuhl–Leibniz-Zentrum fuer Informatik, 2012, pp. 113–122. ISBN: 978-3-939897-46-0. DOI: 10.4230/OASIcs.VLUDS.2011.113. URL: http://drops.dagstuhl.de/opus/volltexte/2012/3745.

[25] Simon Grude et al. “Controlling mobile Spykee robot using Emotiv Neuro headset”. In: *Proceedings of the 32nd Chinese Control Conference* (2013), pp. 5927–5932.

[26] Omamah Hawsawi and Sudhanshu K. Semwal. “EEG headset supporting mobility impaired gamers with game accessibility”. In: *2014 IEEE International Conference on Systems, Man, and Cybernetics (SMC)*. 2014, pp. 837–841. DOI: 10.1109/SMC.2014.6974015.

[27] Rain Ashford. “ThinkerBelle EEG Amplifying Dress”. In: *Adjunct Proceedings of the 2015 ACM International Joint Conference on Pervasive and Ubiquitous Computing and Proceedings of the 2015 ACM International Symposium*

*on Wearable Computers*. UbiComp/ISWC'15 Adjunct. Osaka, Japan: Association for Computing Machinery, 2015, pp. 607–612. ISBN: 9781450335751. DOI: 10.1145/2800835.2801673. URL: https://doi.org/10.1145/2800835.2801673.

[28] Agus Siswoyo, Zainal Arief, and Indra Adji Sulistijono. "Application of Artificial Neural Networks in Modeling Direction Wheelchairs Using Neurosky Mindset Mobile (EEG) Device". In: *EMITTER International Journal of Engineering Technology* 5.1 (July 2017), pp. 170–191. DOI: 10.24003/emitter.v5i1.165. URL: https://emitter2.pens.ac.id/ojs/index.php/emitter/article/view/165.

[29] Martin Steinisch, Maria Gabriella Tana, and Silvia Comani. "A Post-Stroke Rehabilitation System Integrating Robotics, VR and High-Resolution EEG Imaging". In: *IEEE Transactions on Neural Systems and Rehabilitation Engineering* 21.5 (2013), pp. 849–859. DOI: 10.1109/TNSRE.2013.2267851.

[30] Sukun Li, Sung-Hyuk Cha, and Charles C. Tappert. "Biometric Distinctiveness of Brain Signals Based on EEG". In: *2018 IEEE 9th International Conference on Biometrics Theory, Applications and Systems (BTAS)*. 2018, pp. 1–6. DOI: 10.1109/BTAS.2018.8698540.

[31] Daria La Rocca, Patrizio Campisi, and Gaetano Scarano. "EEG biometrics for individual recognition in resting state with closed eyes". In: Sept. 2012.

[32] Jérémy Frey et al. "Scientific Outreach with Teegi, a Tangible EEG Interface to Talk about Neurotechnologies". In: *Proceedings of the 2017 CHI Conference Extended Abstracts on Human Factors in Computing Systems*. CHI EA '17. Denver, Colorado, USA: Association for Computing Machinery, 2017, pp. 405–408. ISBN: 9781450346566. DOI: 10.1145/3027063.3052971. URL: https://doi.org/10.1145/3027063.3052971.

[33] Gautham Raj Vijayaragavan et al. "EEG monitored mind de-stressing smart phone application using Yoga and Music Therapy". In: *2015 International Conference on Green Computing and Internet of Things (ICGCIoT)*. 2015, pp. 412–415. DOI: 10.1109/ICGCIoT.2015.7380498.

[34] Rami N. Khushaba et al. "Consumer neuroscience: Assessing the brain response to marketing stimuli using electroencephalogram (EEG) and eye tracking". In: *Expert Systems with Applications* 40.9 (2013), pp. 3803–3812. ISSN: 0957-4174. DOI: https://doi.org/10.1016/j.eswa.2012.12.095. URL: https://www.sciencedirect.com/science/article/pii/S0957417412013371.

[35] Liwei Hsu and Yen-Jung Chen. “Neuromarketing, Subliminal Advertising, and Hotel Selection: An EEG Study”. In: *Australasian Marketing Journal* 28.4 (2020), pp. 200–208. DOI: 10.1016/j.ausmj.2020.04.009. eprint: https://doi.org/10.1016/j.ausmj.2020.04.009. URL: https://doi.org/10.1016/j.ausmj.2020.04.009.

[36] V. Sakkalis. “Review of advanced techniques for the estimation of brain connectivity measured with EEG/MEG”. In: *Computers in Biology and Medicine* 41.12 (2011), pp. 1110–1117. ISSN: 00104825. DOI: 10.1016/j.compbiomed.2011.06.020. URL: http://dx.doi.org/10.1016/j.compbiomed.2011.06.020.

[37] André M. Bastos and Jan Mathijs Schoffelen. “A tutorial review of functional connectivity analysis methods and their interpretational pitfalls”. In: *Frontiers in Systems Neuroscience* 9.JAN2016 (2016), pp. 1–23. ISSN: 16625137. DOI: 10.3389/fnsys.2015.00175.

[38] Stefan J Kiebel et al. “Dynamic causal modelling for EEG and MEG.” eng. In: *Cognitive neurodynamics* 2.2 (June 2008), pp. 121–136. ISSN: 1871-4080 (Print). DOI: 10.1007/s11571-008-9038-0.

[39] John Geweke. “Measurement of linear dependence and feedback between multiple time series”. In: *Journal of the American statistical association* 77.378 (1982), pp. 304–313.

[40] Yuzo Hosoya. “Elimination of third-series effect and defining partial measures of causality”. In: *Journal of Time Series Analysis* 22.5 (2001). Cited by: 41, pp. 537–554. DOI: 10.1111/1467-9892.00240. URL: https://www.scopus.com/inward/record.uri?eid=2-s2.0-0039890223&doi=10.1111%2f1467-9892.00240&partnerID=40&md5=2127e7f751f79bae654d51dad7bc3a88.

[41] John F. Geweke. “Measures of conditional linear dependence and feedback between time series”. In: *Journal of the American Statistical Association* 79.388 (1984). Cited by: 479, pp. 907–915. DOI: 10.1080/01621459.1984.10477110. URL: https://www.scopus.com/inward/record.uri?eid=2-s2.0-84950949120&doi=10.1080%2f01621459.1984.10477110&partnerID=40&md5=d935f170411ed4a91b8a395f7584820b.

[42] Luiz A. Baccalá and Koichi Sameshima. “Partial directed coherence: A new concept in neural structure determination”. In: *Biological Cybernetics* 84.6 (2001). Cited by: 1237, pp. 463–474. DOI: 10.1007/PL00007990. URL: https://www.scopus.com/inward/record.uri?eid=2-s2.0-0035377249&doi=10.1007%2fPL00007990&partnerID=40&md5=d2d4ba4dc0d03a8a66103880ce367537.

[43] Ramesh Srinivasan et al. “EEG and MEG coherence: measures of functional connectivity at distinct spatial scales of neocortical dynamics”. eng. In: *Journal of neuroscience methods* 166.1 (Oct. 2007), pp. 41–52. ISSN: 0165-0270. DOI: 10.1016/j.jneumeth.2007.06.026. URL: https://pubmed.ncbi.nlm.nih.gov/17698205%20https://www.ncbi.nlm.nih.gov/pmc/articles/PMC2151962/.

[44] Narayan P Subramaniyam. *Assessing Connectivity with Phase Locking Value – Sapien Labs | Neuroscience | Human Brain Diversity Project*. 2019. URL: https://sapienlabs.org/lab-talk/phase-locking-value/ (visited on 03/19/2022).

[45] Narayan P Subramaniyam. *Assessing Connectivity with Phase Locking Value*. 2019. URL: https://sapienlabs.org/phase-locking-value/ (visited on 12/19/2021).

[46] Menorca Chaturvedi et al. “Phase lag index and spectral power as QEEG features for identification of patients with mild cognitive impairment in Parkinson’s disease”. In: *Clinical Neurophysiology* 130.10 (2019), pp. 1937–1944. ISSN: 1388-2457. DOI: https://doi.org/10.1016/j.clinph.2019.07.017. URL: https://www.sciencedirect.com/science/article/pii/S1388245719311630.

[47] Kenji Marshall, Charlotte Maschke, and Stefanie Blain-Moraes. *Comparing PLI, wPLI, and dPLI — MNE-Connectivity 0.4.0 documentation*. URL: https://mne.tools/mne-connectivity/stable/auto_examples/dpli_wpli_pli.html.

[48] Kara J. Pavone et al. “Nitrous oxide-induced slow and delta oscillations”. In: *Clinical Neurophysiology* 127.1 (2016), pp. 556–564. ISSN: 18728952. DOI: 10.1016/j.clinph.2015.06.001. URL: http://dx.doi.org/10.1016/j.clinph.2015.06.001.

[49] Edmond I. Eger II et al. “Hypothesis: Inhaled anesthetics produce immobility and amnesia by different mechanisms at different sites”. In: *Anesthesia and Analgesia* 84.4 (1997), pp. 915–918. DOI: 10.1097/00000539-199704000-00039. URL: https://www.scopus.com/inward/record.uri?eid=2-s2.0-0030934678&doi=10.1097%2f00000539-199704000-00039&partnerID=40&md5=5125a8210bfacd7210e5ab2887af9a20.

[50] Levin Kuhlmann, Brett L Foster, and David T J Liley. “Modulation of functional EEG networks by the NMDA antagonist nitrous oxide.” eng. In: *PloS one* 8.2 (2013), e56434. ISSN: 1932-6203 (Electronic). DOI: 10.1371/journal.pone.0056434.

[51] The Investopedia Team. *Statistical Significance Definition: Types and How It's Calculated*. 2021. URL: https://www.investopedia.com/terms/s/statistical-significance.asp (visited on 08/01/2022).

[52] Peter Dalgaard. "Power and the computation of sample size". In: *Introductory Statistics with R*. New York, NY: Springer New York, 2008, pp. 155–162. ISBN: 978-0-387-79054-1. DOI: 10.1007/978-0-387-79054-1_9. URL: https://doi.org/10.1007/978-0-387-79054-1_9.

[53] Aleksandra Miljevic et al. *EEG-connectivity: A fundamental guide and checklist for optimal study design and evaluation*. 2021. DOI: 10.48550/ARXIV.2108.13611. URL: https://arxiv.org/abs/2108.13611.

[54] Andrew Zalesky, Alex Fornito, and Edward T. Bullmore. "Network-based statistic: Identifying differences in brain networks". In: *NeuroImage* 53.4 (2010), pp. 1197–1207. ISSN: 1053-8119. DOI: https://doi.org/10.1016/j.neuroimage.2010.06.041. URL: https://www.sciencedirect.com/science/article/pii/S1053811910008852.

[55] Mike X Cohen. *Analyzing Neural Time Series Data: Theory and Practice*. The MIT Press, Jan. 2014. ISBN: 9780262319553. DOI: 10.7551/mitpress/9609.001.0001. URL: https://doi.org/10.7551/mitpress/9609.001.0001.

[56] Mainak Jas et al. "Autoreject: Automated artifact rejection for MEG and EEG data". In: *NeuroImage* 159.June (2017), pp. 417–429. ISSN: 10959572. DOI: 10.1016/j.neuroimage.2017.06.030. arXiv: 1612.08194. URL: https://doi.org/10.1016/j.neuroimage.2017.06.030.

[57] Erick Ortiz et al. "Weighted phase lag index and graph analysis: Preliminary investigation of functional connectivity during resting state in children". In: *Computational and Mathematical Methods in Medicine* 2012.September (2012). ISSN: 17486718. DOI: 10.1155/2012/186353.

[58] Junfeng Sun, Xiangfei Hong, and Shanbao Tong. "Phase synchronization analysis of eeg signals: An evaluation based on surrogate tests". In: *IEEE Transactions on Biomedical Engineering* 59.8 (2012), pp. 2254–2263. ISSN: 00189294. DOI: 10.1109/TBME.2012.2199490.

[59] Aaron J Newman. *Artifacts in EEG Data — Data Science for Psychology and Neuroscience — in Python*. 2020. URL: https://neuraldatascience.io/7-eeg/erp_artifacts.html.

[60] Patricia Fernández-Palleiro et al. “Brainwaves Oscillations as a Potential Biomarker for Major Depression Disorder Risk”. In: *Clinical EEG and Neuroscience* 51.1 (2020). PMID: 31537100, pp. 3–9. DOI: 10.1177/1550059419876807. eprint: https://doi.org/10.1177/1550059419876807. URL: https://doi.org/10.1177/1550059419876807.

[61] Matteo Demuru et al. “A comparison between power spectral density and network metrics: An EEG study”. In: *Biomedical Signal Processing and Control* 57 (2020), p. 101760. ISSN: 1746-8094. DOI: https://doi.org/10.1016/j.bspc.2019.101760. URL: https://www.sciencedirect.com/science/article/pii/S1746809419303416.

[62] Babak Mohammadzadeh, Kazem Sattari, and Masoud Lotfizadeh. “Determining the relationship between depression and brain waves in depressed subjects using Pearson correlation and regression”. In: *International Journal of Epidemiologic Research* 3.4 (2016), pp. 376–385. ISSN: 2383-4366. eprint: http://ijer.skums.ac.ir/article_23155_dcd57e60b454052f16b09a2d1ac82d90.pdf. URL: http://ijer.skums.ac.ir/article_23155.html.

[63] Margherita Lai et al. “A comparison between scalp- and source-reconstructed EEG networks”. In: *Scientific Reports* 8 (1 Dec. 2018). ISSN: 20452322. DOI: 10.1038/s41598-018-30869-w.

[64] Jan-Mathijs Schoffelen and Joachim Gross. “Source connectivity analysis with MEG and EEG”. In: *Human brain mapping* 30.6 (2009), pp. 1857–1865.

[65] Garcia Dominguez Luis et al. “Enhanced measured synchronization of unsynchronized sources: inspecting the physiological significance of synchronization analysis of whole brain electrophysiological recordings”. In: *International Journal of Physical Sciences* 2.11 (2007), pp. 305–317.

# APPENDIX A. Circular graphs

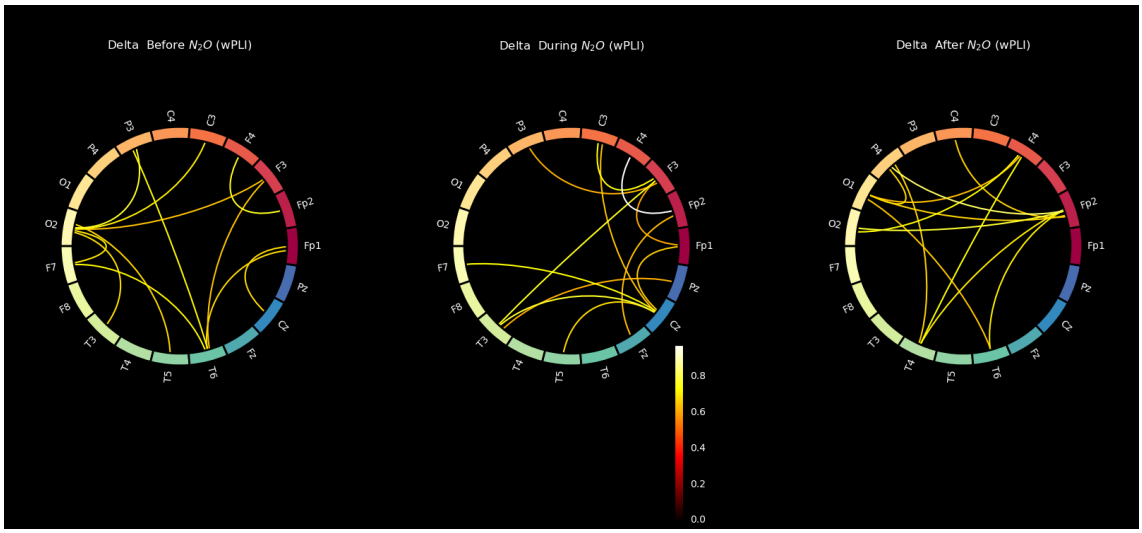


***Figure 1*** *Circular connectivity graph of subject 4 (from the continuous group) in the delta band showing the 12 strongest connectivity strengths between pairs of electrodes in episodes of before, during and after nitrous oxide anaesthesia.*

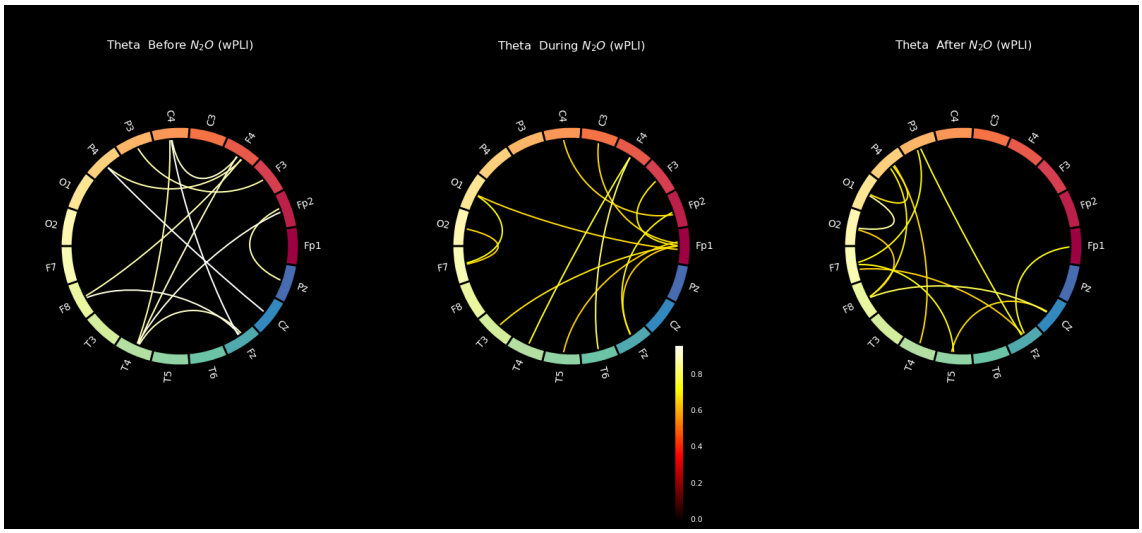


***Figure 2*** *Circular connectivity graph of subject 4 (from the continuous group) in the theta band showing the 12 strongest connectivity strengths between pairs of electrodes in episodes of before, during and after nitrous oxide anaesthesia.*

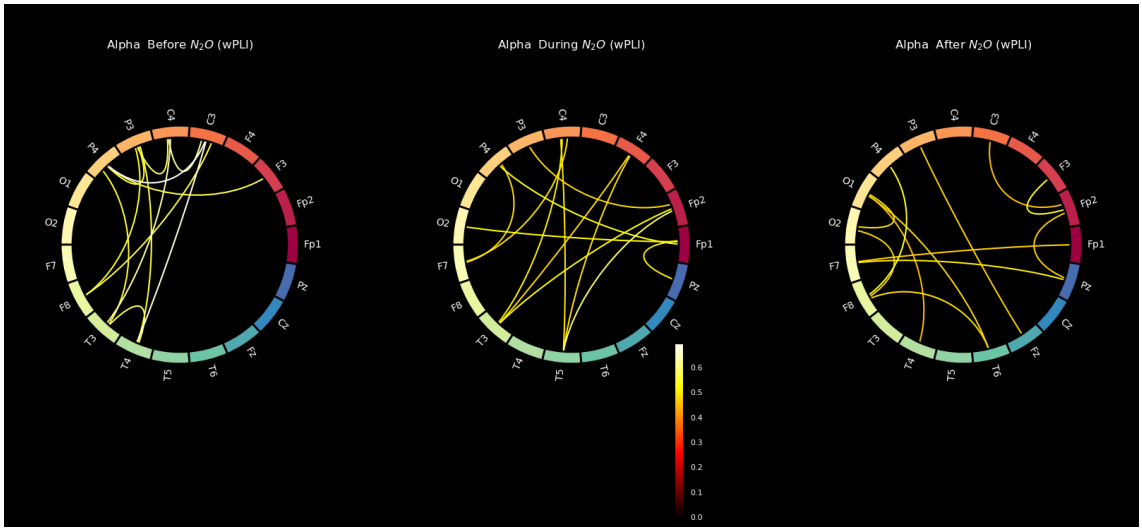


***Figure 3*** *Circular connectivity graph of subject 4 (from the continuous group) in the alpha band showing the 12 strongest connectivity strengths between pairs of electrodes in episodes of before, during and after nitrous oxide anaesthesia.*

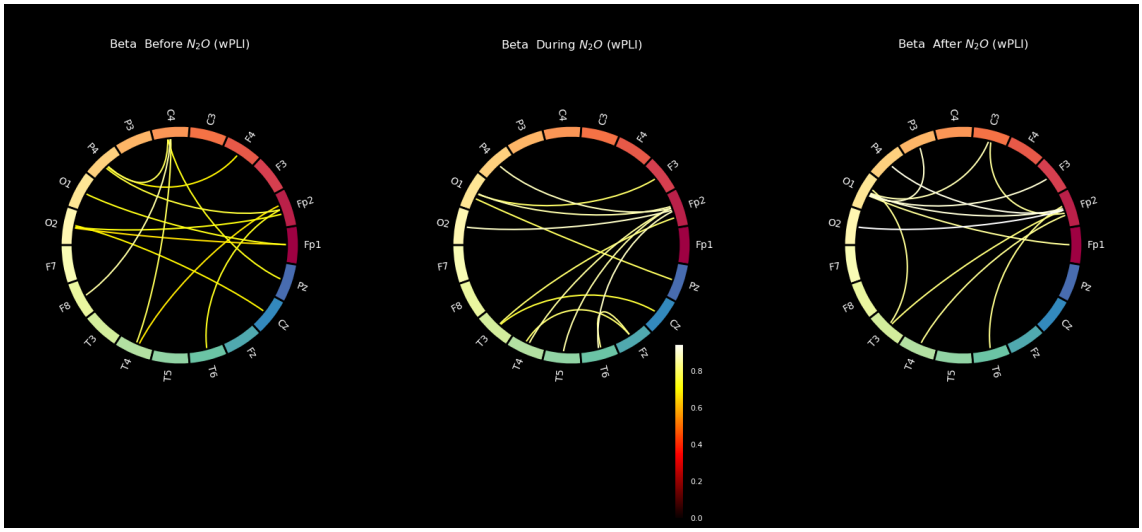


***Figure 4*** *Circular connectivity graph of subject 4 (from the continuous group) in the beta band showing the 12 strongest connectivity strengths between pairs of electrodes in episodes of before, during and after nitrous oxide anaesthesia.*

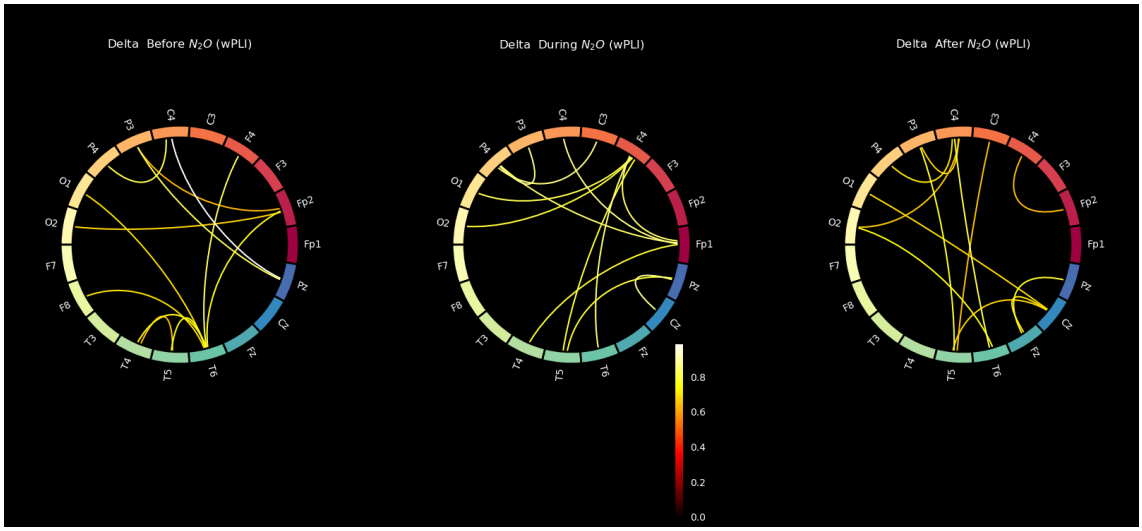


***Figure 5*** *Circular connectivity graph of subject 7 (from the continuous group) in the delta band showing the 12 strongest connectivity strengths between pairs of electrodes in episodes of before, during and after nitrous oxide anaesthesia.*

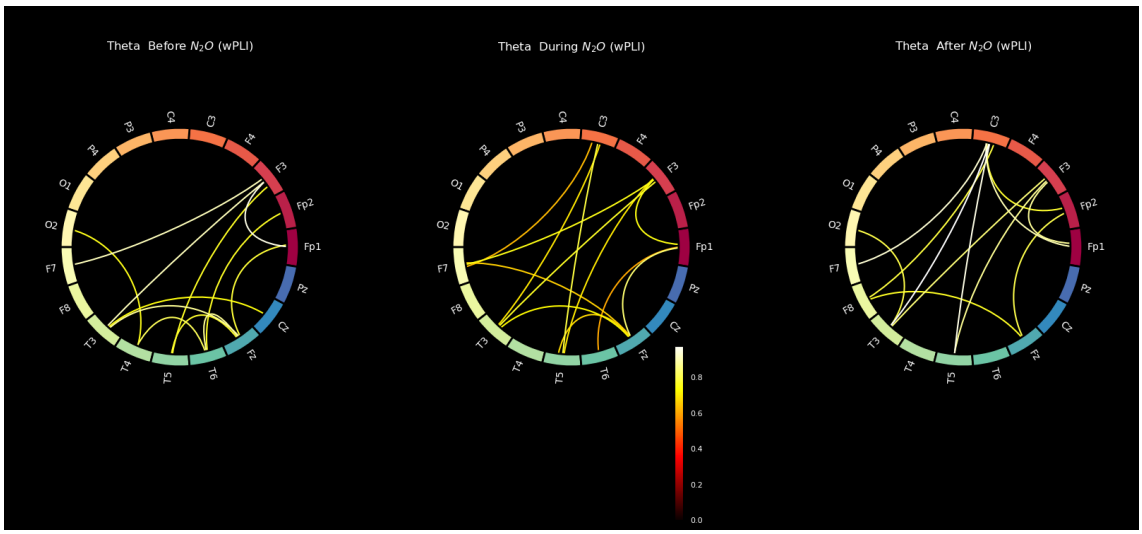


***Figure 6*** *Circular connectivity graph of subject 7 (from the continuous group) in the theta band showing the 12 strongest connectivity strengths between pairs of electrodes in episodes of before, during and after nitrous oxide anaesthesia.*

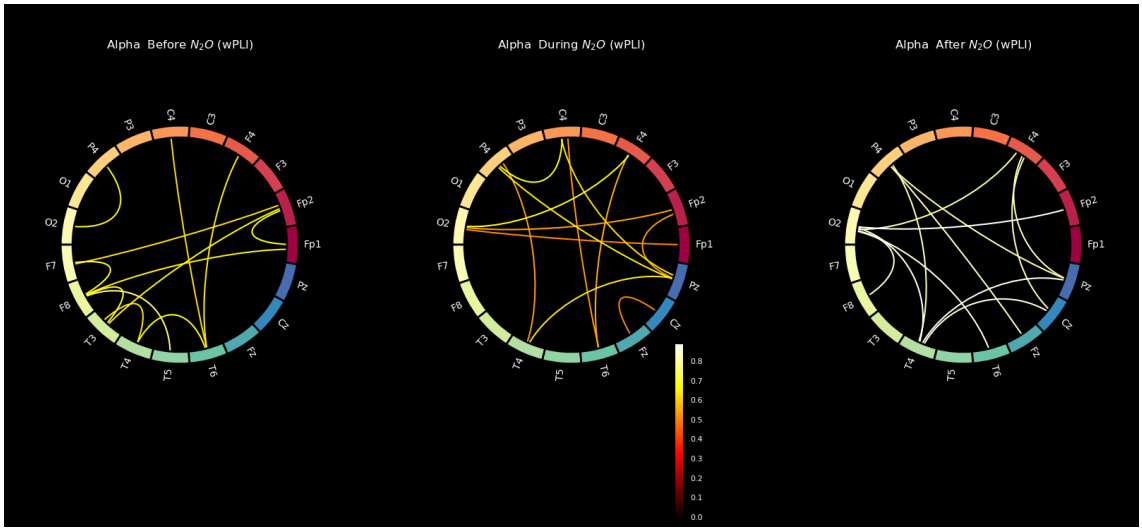


***Figure 7*** *Circular connectivity graph of subject 7 (from the continuous group) in the alpha band showing the 12 strongest connectivity strengths between pairs of electrodes in episodes of before, during and after nitrous oxide anaesthesia.*

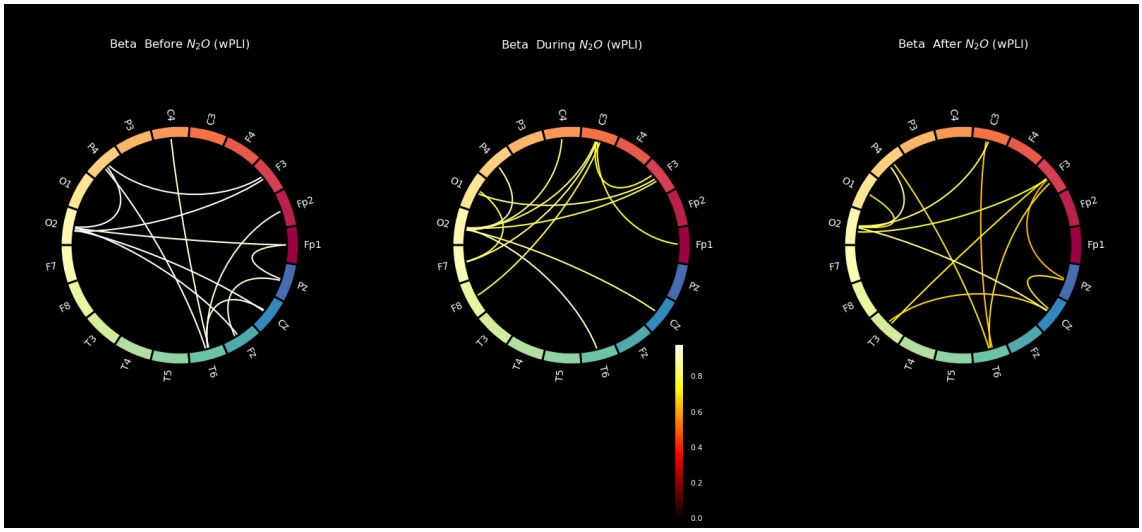


***Figure 8*** *Circular connectivity graph of subject 7 (from the continuous group) in the beta band showing the 12 strongest connectivity strengths between pairs of electrodes in episodes of before, during and after nitrous oxide anaesthesia.*

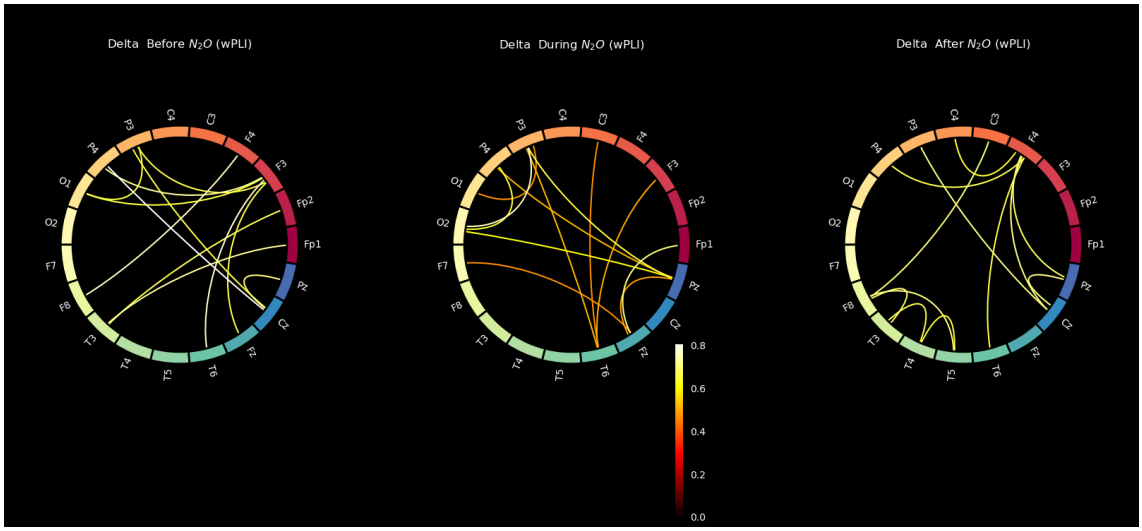


***Figure 9*** *Circular connectivity graph of subject 11 (from the continuous group) in the delta band showing the 12 strongest connectivity strengths between pairs of electrodes in episodes of before, during and after nitrous oxide anaesthesia.*

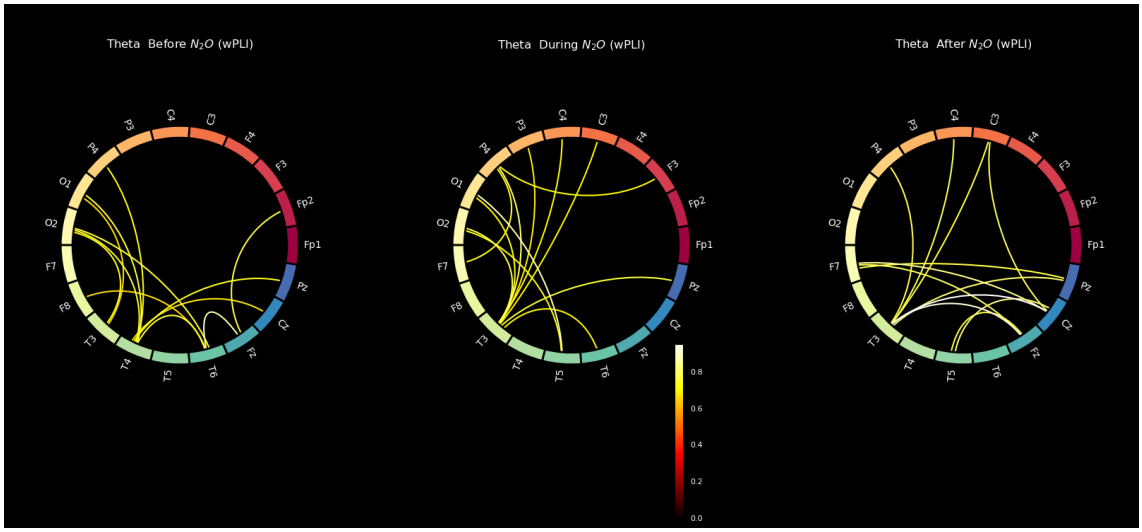


***Figure 10*** *Circular connectivity graph of subject 11 (from the continuous group) in the theta band showing the 12 strongest connectivity strengths between pairs of electrodes in episodes of before, during and after nitrous oxide anaesthesia.*

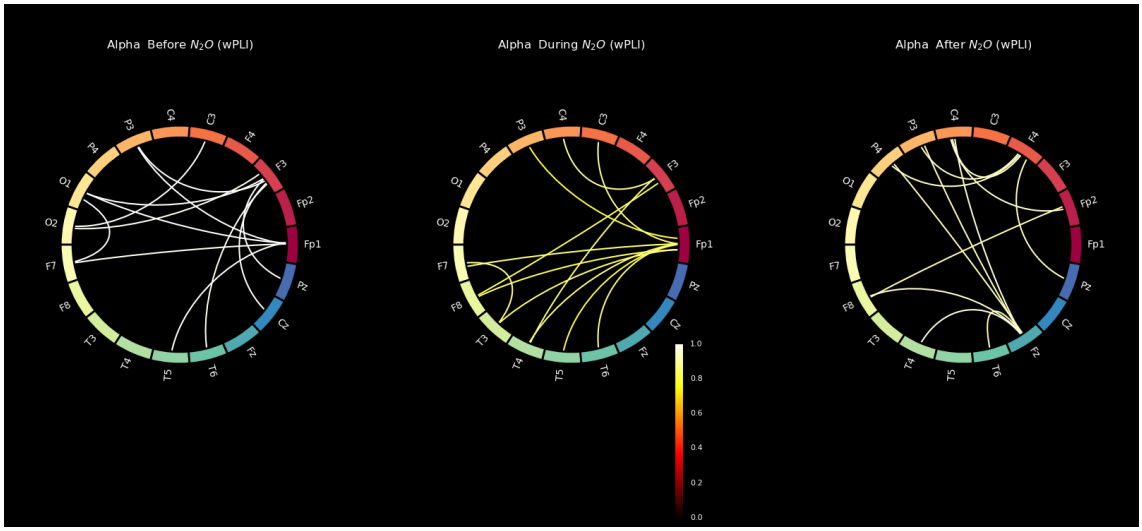


***Figure 11*** *Circular connectivity graph of subject 11 (from the continuous group) in the alpha band showing the 12 strongest connectivity strengths between pairs of electrodes in episodes of before, during and after nitrous oxide anaesthesia.*

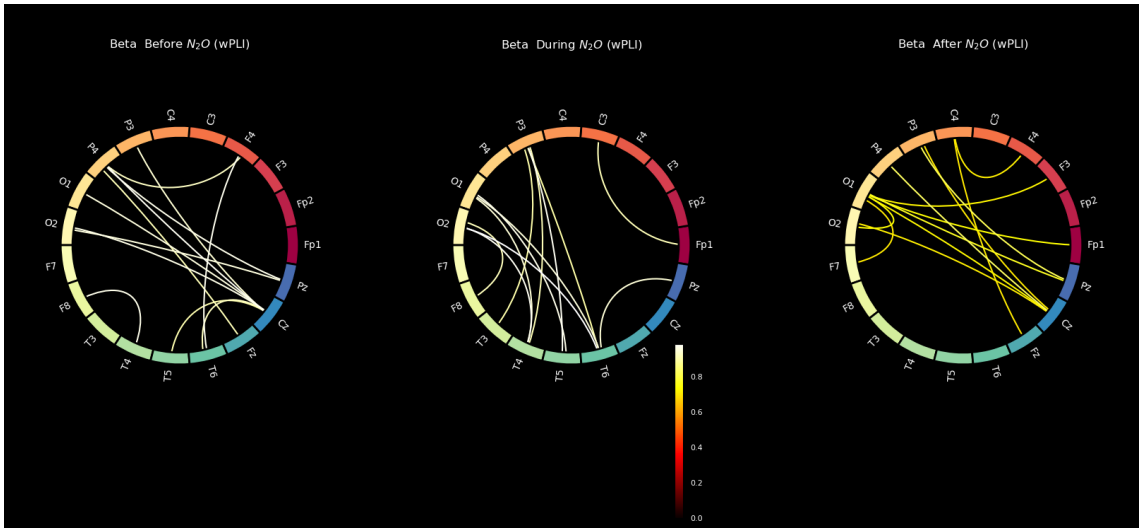


***Figure 12*** *Circular connectivity graph of subject 11 (from the continuous group) in the beta band showing the 12 strongest connectivity strengths between pairs of electrodes in episodes of before, during and after nitrous oxide anaesthesia.*

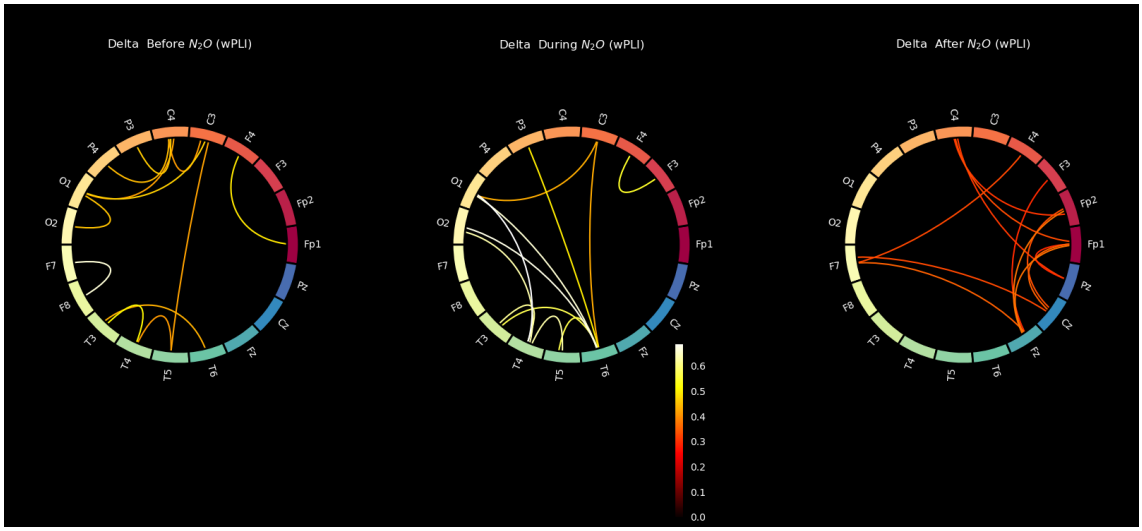


***Figure 13*** *Circular connectivity graph of subject 19 (from the continuous group) in the delta band showing the 12 strongest connectivity strengths between pairs of electrodes in episodes of before, during and after nitrous oxide anaesthesia.*

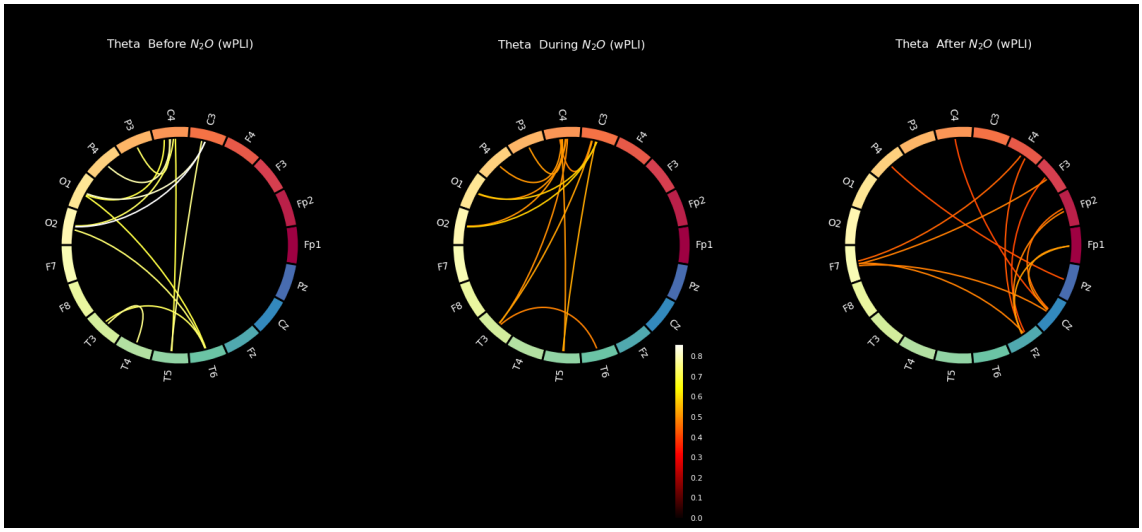


***Figure 14*** *Circular connectivity graph of subject 19 (from the continuous group) in the theta band showing the 12 strongest connectivity strengths between pairs of electrodes in episodes of before, during and after nitrous oxide anaesthesia.*

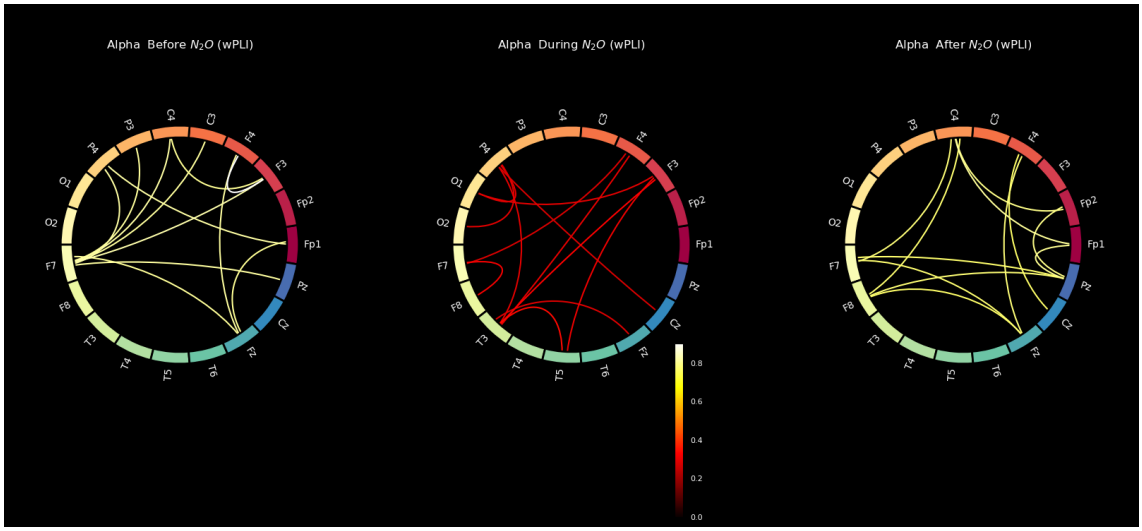


***Figure 15*** *Circular connectivity graph of subject 19 (from the continuous group) in the alpha band showing the 12 strongest connectivity strengths between pairs of electrodes in episodes of before, during and after nitrous oxide anaesthesia.*

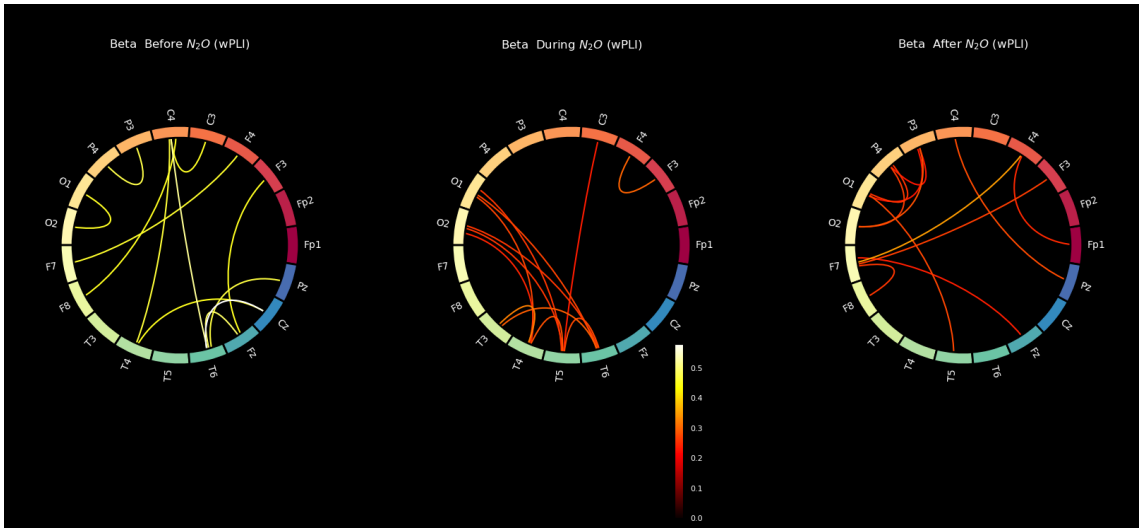


***Figure 16*** *Circular connectivity graph of subject 19 (from the continuous group) in the beta band showing the 12 strongest connectivity strengths between pairs of electrodes in episodes of before, during and after nitrous oxide anaesthesia.*

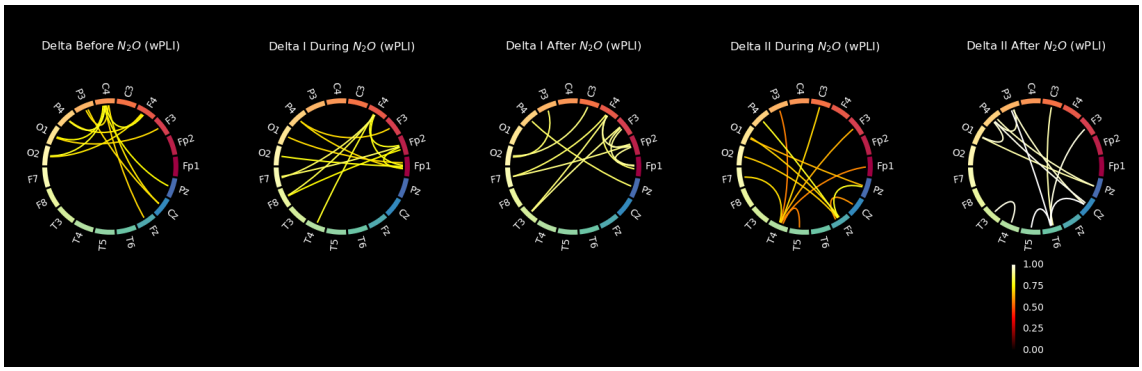


***Figure 17*** *Circular connectivity graph of subject 13 (from the intermittent group) in the delta band showing the 12 strongest connectivity strengths between pairs of electrodes in episodes of before, during1, after1, during2 and after2 nitrous oxide anaesthesia.*

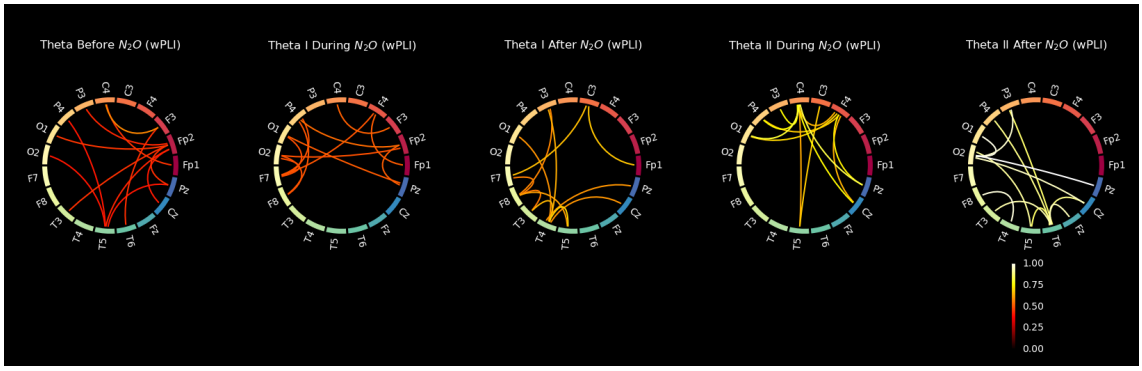


***Figure 18*** *Circular connectivity graph of subject 13 (from the intermittent group) in the theta band showing the 12 strongest connectivity strengths between pairs of electrodes in episodes of before, during1, after1, during2 and after2 nitrous oxide anaesthesia.*

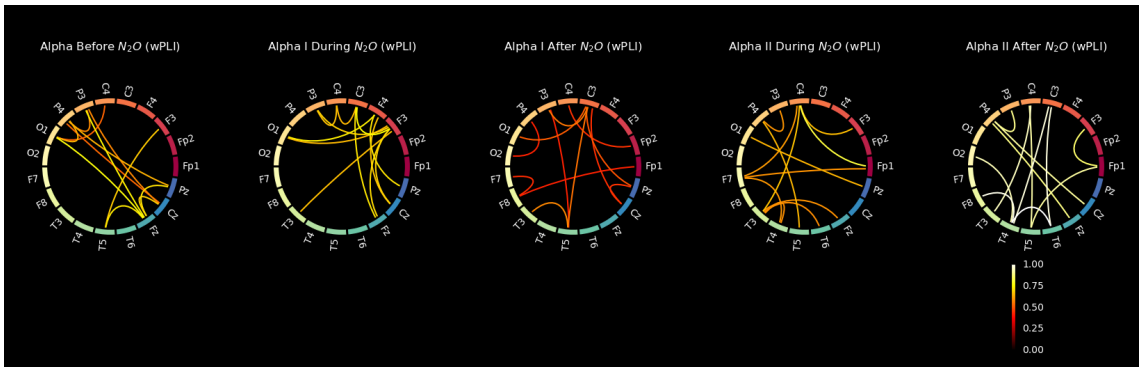


***Figure 19*** *Circular connectivity graph of subject 13 (from the intermittent group) in the alpha band showing the 12 strongest connectivity strengths between pairs of electrodes in episodes of before, during1, after1, during2 and after2 nitrous oxide anaesthesia.*

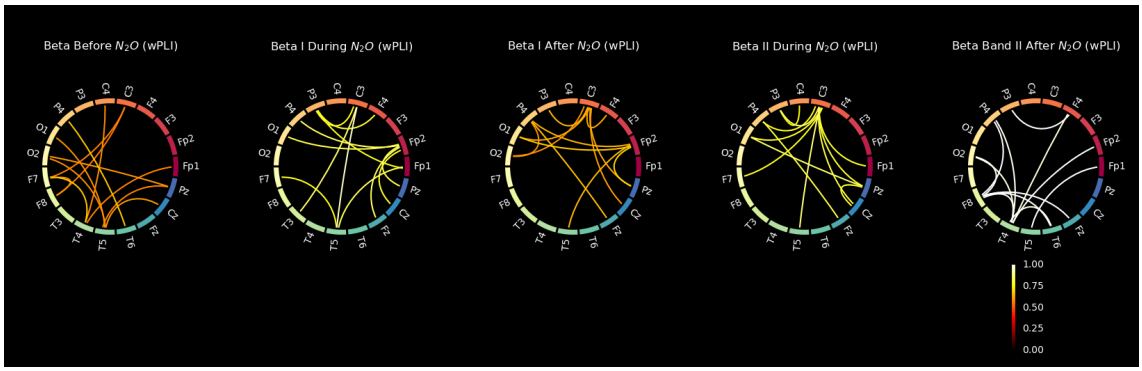


***Figure 20*** *Circular connectivity graph of subject 13 (from the intermittent group) in the beta band showing the 12 strongest connectivity strengths between pairs of electrodes in episodes of before, during1, after1, during2 and after2 nitrous oxide anaesthesia.*


***Figure 21*** *Circular connectivity graph of subject 14 (from the intermittent group) in the delta band showing the 12 strongest connectivity strengths between pairs of electrodes in episodes of before, during1, after1, during2 and after2 nitrous oxide anaesthesia.*

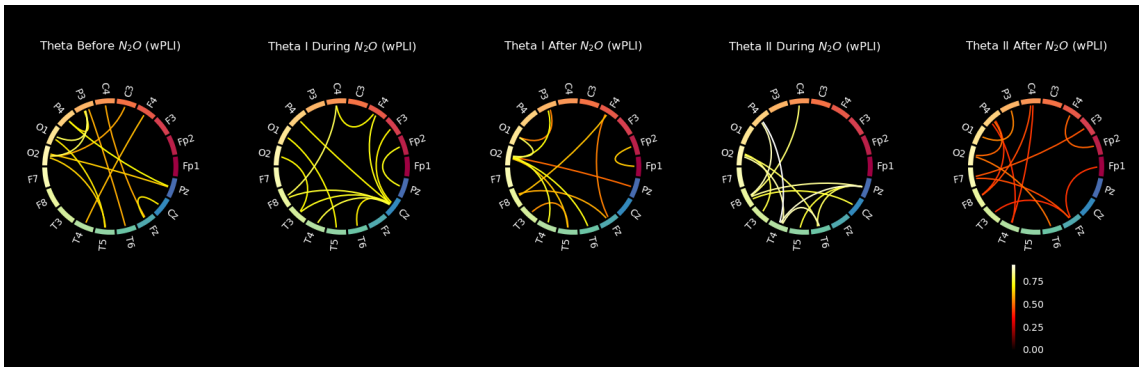


***Figure 22*** *Circular connectivity graph of subject 14 (from the intermittent group) in the theta band showing the 12 strongest connectivity strengths between pairs of electrodes in episodes of before, during1, after1, during2 and after2 nitrous oxide anaesthesia.*

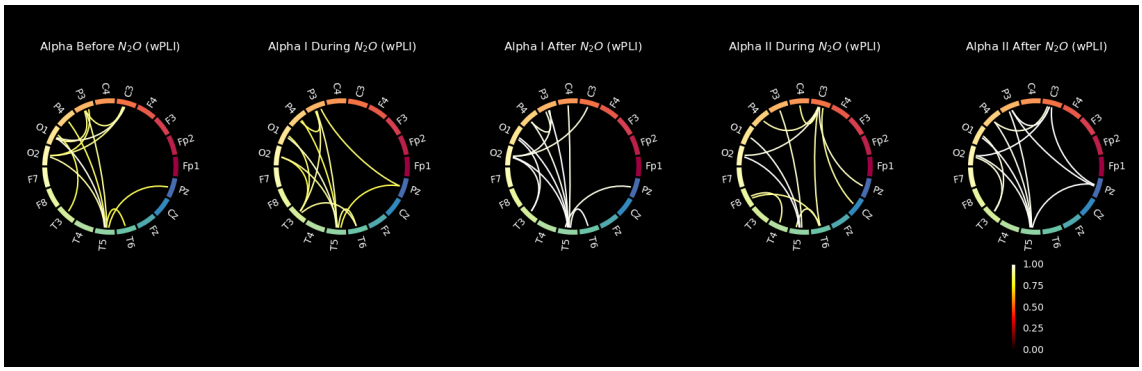


***Figure 23*** *Circular connectivity graph of subject 14 (from the intermittent group) in the alpha band showing the 12 strongest connectivity strengths between pairs of electrodes in episodes of before, during1, after1, during2 and after2 nitrous oxide anaesthesia.*

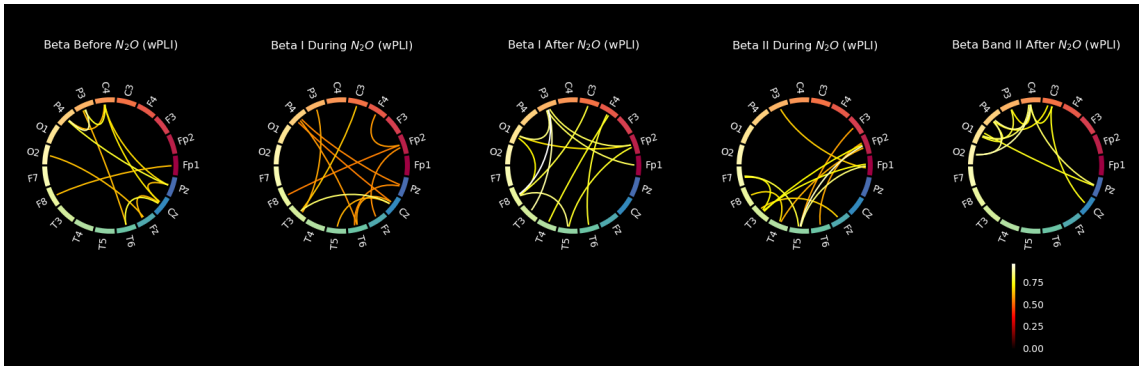


***Figure 24*** *Circular connectivity graph of subject 14 (from the intermittent group) in the beta band showing the 12 strongest connectivity strengths between pairs of electrodes in episodes of before, during1, after1, during2 and after2 nitrous oxide anaesthesia.*


***Figure 25*** *Circular connectivity graph of subject 18 (from the intermittent group) in the delta band showing the 12 strongest connectivity strengths between pairs of electrodes in episodes of before, during1, after1, during2 and after2 nitrous oxide anaesthesia.*

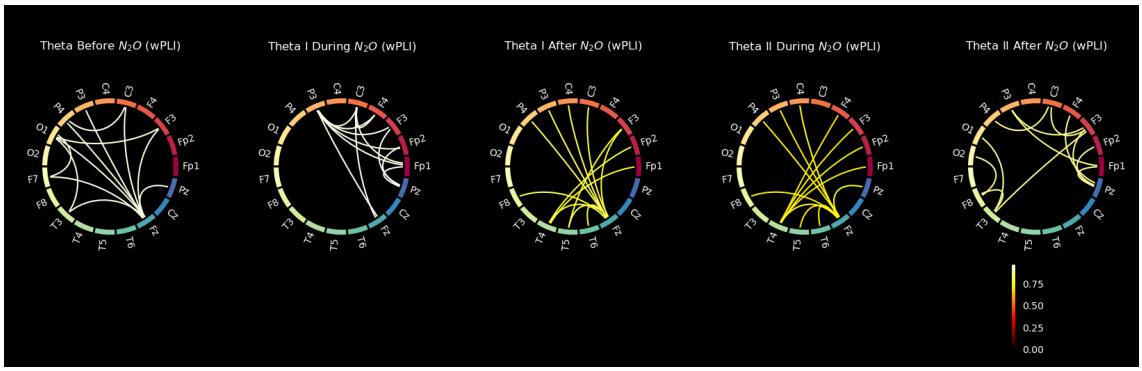


***Figure 26*** *Circular connectivity graph of subject 18 (from the intermittent group) in the theta band showing the 12 strongest connectivity strengths between pairs of electrodes in episodes of before, during1, after1, during2 and after2 nitrous oxide anaesthesia.*

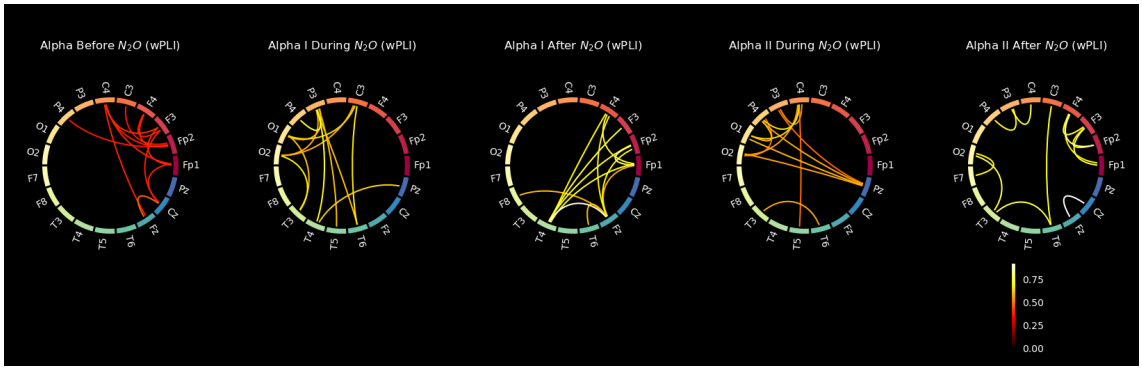


***Figure 27*** *Circular connectivity graph of subject 18 (from the intermittent group) in the alpha band showing the 12 strongest connectivity strengths between pairs of electrodes in episodes of before, during1, after1, during2 and after2 nitrous oxide anaesthesia.*

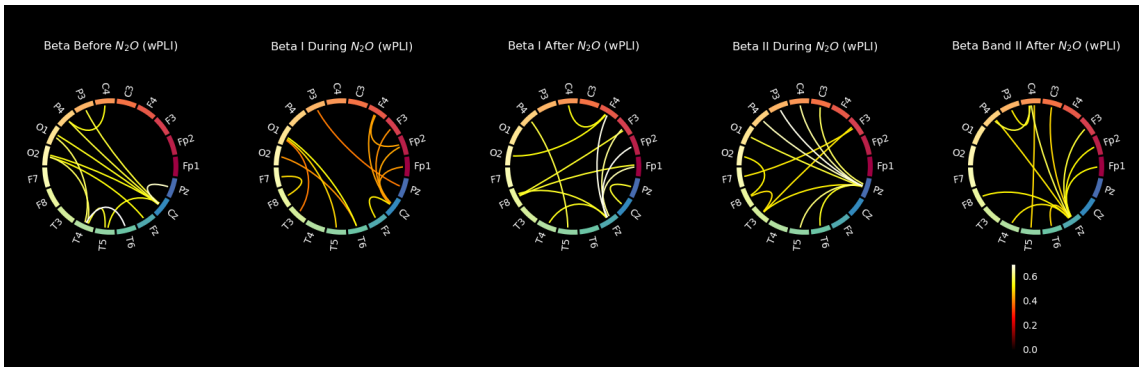


***Figure 28*** *Circular connectivity graph of subject 18 (from the intermittent group) in the theta band showing the 12 strongest connectivity strengths between pairs of electrodes in episodes of before, during1, after1, during2 and after2 nitrous oxide anaesthesia.*

# APPENDIX B. Algorithms

The GitHub links below contain the Python scripts used to preprocess the EEG data and other analyses performed in this thesis work.

*EEG-Preprocessing pipeline*
*Analysis scripts in Python*